

# Energy flow and fluctuations in non-equilibrium conformal field theory on star graphs

Benjamin Doyon<sup>♠</sup>, Marianne Hoogeveen<sup>♠</sup> and Denis Bernard<sup>♣</sup>

<sup>♠</sup> Department of Mathematics, King's College London, London, United Kingdom.

<sup>♣</sup> Laboratoire de Physique Théorique de l'ENS, CNRS & Ecole Normale Supérieure de Paris, France.

We consider non-equilibrium quantum steady states in conformal field theory (CFT) on star-graph configurations, with a particular, simple connection condition at the vertex of the graph. These steady states occur after a large time as a result of initially thermalizing the legs of the graph at different temperatures, and carry energy flows. Using purely Virasoro algebraic calculations we evaluate the exact scaled cumulant generating function for these flows. We show that this function satisfies a generalization of the usual non-equilibrium fluctuation relations. This extends the results by two of the authors (J. Phys. A 45: 362001, 2012; arXiv:1302.3125) to the cases of more than two legs. It also provides an alternative derivation centered on Virasoro algebra operators rather than local fields, hence an alternative regularization scheme, thus confirming the validity and universality of the scaled cumulant generating function. Our derivation shows how the usual Virasoro algebra leads, in large volumes, to a continuous-index Virasoro algebra for which we develop diagrammatic principles, which may be of interest in other non-equilibrium contexts as well. Finally, our results shed light on the Poisson process interpretation of the long-time energy transfer in CFT.

November 11, 2018

## 1 Introduction

There is currently great interest in the thermodynamics of quantum systems out of equilibrium. This has to do in part with the general need to find a framework that extends equilibrium thermodynamics to far-from-equilibrium situations [1], and in part with the recent experimental advances which make it possible to prepare quantum systems in non-equilibrium states in a controlled way, and verify fluctuation relations experimentally [2, 3, 4, 5, 6]. In the context of non-equilibrium quantum steady states, where there is transfer of energy, charge, particles, etc., one of the objects of interest is the scaled cumulant generating function (the Legendre transform of the large-deviation function), see for instance the review [7]. This characterizes the fluctuations of these transfers measured over a large time period, and encodes many properties of their non-equilibrium statistics. Calculating it exactly in model systems and obtaining the associated fluctuation relations are important steps in developing the general theory of non-equilibrium steady states.

Recently, a step in this direction was achieved by calculating exactly the scaled cumulant generating function in non-equilibrium conformal field theory (NECFT) [8, 9], for energy and charge transfer. The setup consisted of two systems (acting as baths), initially thermalized at different temperatures and chemical potentials, that were connected to form a homogeneous system, so that a steady state is established at late times. Besides deriving the non-equilibrium density matrix and proving an exact nontrivial formula for the cumulant generating function in this relatively simple situation of NECFT, two claims were made. Firstly, it was claimed (with justifications) in [8, 9] that this formula is *universal*. That is, it gives the correct scaled cumulant generating function for any quantum critical system<sup>1</sup>, prepared in the way described above, at small temperatures and chemical potentials.<sup>2</sup> This is a nontrivial statement, meaning that for the first time, the exact long-time fluctuation statistics were obtained for both energy and charge transfer for many families of

<sup>1</sup>With dynamical critical exponent  $z = 1$ .

<sup>2</sup>There are subtleties regarding the interplay between the large- $t$  limit and the scaling limit. These are discussed in [9].

quantum systems, even with very strong interactions. The only parameter needed, that encodes the interaction, is the central charge. The NECFT universal average current was recently confirmed numerically [10] in a particular critical quantum model. It was also observed in [8] that the long-time energy transfer statistics is purely Poissonian, leading to the claim that the natural right-moving and left-moving energy carriers behave over a long time like ensembles of Poissonian particles.

The objective of the present paper is two-fold. Firstly, we generalize the results of [8] to non-equilibrium energy flows amongst any number of baths, connected to each other at one point in a star-graph configuration. We obtain the density matrix and derive the exact universal scaled cumulant generating function (which we will sometimes refer to as the full counting statistics) in NECFT under a simple connection condition at the vertex of the graph. Our results are a simple generalization of those of [8], and we find a generalization of the standard fluctuation relations to this many-leg case. There has been a lot of activity in the study of such “quantum graphs” (see for instance [11] for a review, and [12, 13, 14, 15, 16, 17, 18, 19] for condensed matter applications). Recently, certain quantum field theory methods and concepts have been introduced (see e.g. [20, 21, 22, 23, 24, 25, 26]) and studies have looked at far-from-equilibrium quantities in various types of quantum graphs [16, 27, 28, 29]. However, to our knowledge no exact cumulant generating function has been derived yet, and most of these studies are restricted to free propagation in the legs of the graph (e.g. Luttinger liquids), concentrating on the nontrivial scattering at vertices (see for instance the methods developed in [30]). By contrast our results apply to general CFT in the legs, possibly representing strongly interacting critical systems, albeit with simple vertex scattering.

Secondly, we develop a new method for deriving the scaled cumulant generating function. Some of the problems in using conformal field theory (CFT) methods in NECFT are that (1) in order to describe baths, the systems must be of infinite length, and (2) there is (yet) no simple Euclidean-space geometry to re-interpret out of equilibrium states and their fluctuations, so that we have a truly real-time problem where the quantization scheme is fixed *a priori*. This hampers the use of standard techniques based on the Virasoro algebra and its representations, which usually require the choice of a quantization scheme where space is compact. This problem was circumvented in [8] by concentrating on the algebra of local fields on the line. Here we attack the problem directly, and develop a method to calculate quantum averages of Virasoro generators in the limit where the length of the system goes to infinity. To that end, we study a continuous-index Virasoro algebra and develop associated diagrammatic principles. This algebraic method could find applications in other contexts, for instance in the study of non-equilibrium steady states in NECFT with nontrivial impurities (impurities are usually described in terms of the Virasoro algebra), or in quantum quenches.

Besides obtaining the non-equilibrium density matrix and deriving the exact scaled cumulant generating function in NECFT with the present simple star-graph configuration, our results provide further evidence for the two claims mentioned above. Indeed, within our new calculation method, there is a natural UV regularization scheme, closely linked to the usual UV regularization of quantum field theory, but different from that used in [9]. Since our results agree with those of [8, 9] in the two-leg case, this provides further confirmation of the expected independence from the regularization scheme, and consequently universality (although it is not a full proof or a full analysis of the effect of irrelevant operators). Also, our cumulant generating function has a clear Poisson-process interpretation further confirming the interpretation of [8].

The paper is organized as follows. In Section 2, we describe precisely the system under consideration and obtain the non-equilibrium density matrix. In Section 3, we describe our main results and discuss their meaning. In Section 4, we develop some aspects of the continuous Virasoro algebra; in particular, we study the diagrams used to evaluate averages. In Section 5 we evaluate the full counting statistics. Finally, in Section 6, we provide concluding remarks.

## 2 A nonequilibrium steady state on a star graph

Consider a number  $N$  of identical, decoupled one-dimensional quantum systems, each of length  $R/2$  and at criticality, thermalized at inverse temperatures  $\beta_1, \dots, \beta_N$ . Assume that the temperatures are

small as compared with the microscopic energy scale  $J$  (the typical energy of a link in a quantum chain, for instance),  $k_B T \ll J$ . Then the physics of each quantum system can be described by a conformal field theory (CFT), with some central charge  $c$ . In particular, the boundaries are also conformal. Since the systems are described by a CFT, the energy and momentum densities (and their descendants), in the bulk, separate into left- and right-movers. We arrange the systems radially, forming the legs (or edges) of a star graph ( $N$  legs meeting at a single vertex); then it is clearer to call the fields incoming or outgoing, where incoming fields are the fields that move towards the vertex, and outgoing are those that move away from the vertex. We will denote them by  $h_j^{\text{in/out}}$ , respectively, so that the energy density is  $h_j^{\text{in}} + h_j^{\text{out}}$  and the (inward) momentum density is  $h_j^{\text{in}} - h_j^{\text{out}}$  in leg  $j$ . Thanks to the conformal boundary conditions, at the boundaries of each system, we have reflective conditions for the densities  $h_j^{\text{in/out}}$  [31]. For example, incoming fields become outgoing fields moving at the same speed upon reaching the innermost boundaries of the systems, which are located at the vertex of the star graph.

At some time  $-t_0 < 0$  in the far past, the independently thermalized systems are all connected at the vertex. There are several ways of making this connection; in this paper the connection is assumed to be made in such a way that the incoming and the outgoing fields on one leg are connected to different legs. More precisely, the incoming fields of the  $j$ -th leg, when they reach the vertex, move into the  $j+1$ -th leg (mod  $N$ ), where they become outgoing fields. One way to think of this connection where incoming and outgoing fields move into different legs is by considering these fields as the edge currents of a set of  $N$  very long and narrow quantum Hall slabs arranged into a star graph.

After the systems are connected, the new total system is evolved unitarily. Then, energy will begin to flow from higher-temperatures regions to lower-temperature regions. If we let the system evolve for a long enough time, we expect the system to reach a steady state. More precisely, in order for the system to be in a steady state at time  $t = 0$ , we must take the length  $R$  to infinity before we take the limit  $t_0 \rightarrow \infty$ . This ensures that the legs of the graph act as reservoirs at different temperatures, and that any finite part of the system around the vertex can be seen as an open system. Indeed, waves emanating from the vertex will not have time to bounce back at outer boundaries, hence will effectively be absorbed by the legs; and waves incoming to the vertex can only come from deep inside the legs, carrying the information of the initial thermalization. We will call this limit,  $\lim_{R \gg t_0 \rightarrow \infty}$ , the steady state limit, and what we mean by the system reaching a steady state is the existence of the limit on averages,

$$\lim_{t_0 \rightarrow \infty} \lim_{R \rightarrow \infty} \langle \dots \rangle_{R, t_0} = \langle \dots \rangle^{\text{stat}}, \quad (1)$$

where  $\langle \dots \rangle_{R, t_0}$  represents the average in the finite- $R$  star graph a length of time  $t_0$  after the connection has been made. Since it is only finite parts around the vertex that are expected to possess a steady state limit, for the system to be said to reach a steady state we only impose this limit to exist whenever the ellipses  $\dots$  are replaced by operators supported in finite regions around the vertex; and in fact, we will here only look at operators in the same Virasoro sector as that of the energy and momentum densities. We expect there to be a steady energy current flowing, so that, in particular, the steady-state average of the energy-current observable (the momentum density) should be finite and nonzero. Note that any finite region around the vertex, no matter how large, will be in a steady state in this limit. What effectively happens in the steady state limit, is that the region in which we have a steady energy current becomes infinitely large, and that the thermal baths are pushed to infinity.

The distance along the any one of the  $N$  legs is parametrized by  $x \in [0, \frac{R}{2}]$ . Before the connection, the continuity conditions for the incoming and outgoing densities  $h^{\text{in/out}}(x)$  are

$$h_j^{\text{in}}(0) = h_j^{\text{out}}(0), \quad h_j^{\text{out}}(\frac{R}{2}) = h_j^{\text{in}}(\frac{R}{2}) \quad (2)$$

and after the connection, these conditions are changed to

$$h_j^{\text{in}}(0) = h_{j+1}^{\text{out}}(0), \quad h_j^{\text{out}}(\frac{R}{2}) = h_j^{\text{in}}(\frac{R}{2}) \quad (3)$$

where here and in the following we understand that leg indices are defined mod  $(N)$ .

The former set of continuity conditions holds under time evolution of the disconnected system, and in averages with the initial state where each system is independently thermalized. The latter set holds under time evolution of the connected system, and, as it will turn out, the part of it at  $x = 0$  holds in the steady state average (the part of it at  $x = R/2$  does not make sense because in the steady state  $R$  has been sent to infinity, and we only get averages of local operators around the vertex).

Let us denote by  $H_0^{(j)}$ ,  $j = 1, \dots, N$  the Hamiltonians of the disconnected systems on the legs of the graph. Then the initial density matrix is

$$\rho_0 = \mathbf{n} \left[ e^{-\sum_{j=1}^N \beta_j H_0^{(j)}} \right]$$

where here and below we use the notation  $\mathbf{n}[\rho] = \rho/\text{Tr}(\rho)$ . This density matrix is invariant under the disconnected-system evolution Hamiltonian  $H_0 = \sum_{j=1}^N H_0^{(j)}$ . Assuming that  $R \gg x, |t| > 0$ , the  $H_0$ -evolution, taking into account (2), is given by

$$e^{iH_0 t} h_j^{\text{out}}(x) e^{-iH_0 t} = \begin{cases} h_j^{\text{out}}(x-t) & x-t > 0 \\ h_j^{\text{in}}(t-x) & x-t < 0 \end{cases} \quad (4)$$

$$e^{iH_0 t} h_j^{\text{in}}(x) e^{-iH_0 t} = \begin{cases} h_j^{\text{in}}(x+t) & x+t > 0 \\ h_j^{\text{out}}(-(x+t)) & x+t < 0 \end{cases} \quad (5)$$

On the other hand, let us denote by  $H$  the Hamiltonian of the connected, total system. The  $H$ -evolution, which takes into account the continuity condition (3) at the vertex and assuming again that  $R \gg x, |t| > 0$ , is given by

$$e^{iH t} h_j^{\text{out}}(x) e^{-iH t} = \begin{cases} h_j^{\text{out}}(x-t) & x-t > 0 \\ h_{j-1}^{\text{in}}(t-x) & x-t < 0 \end{cases} \quad (6)$$

$$e^{iH t} h_j^{\text{in}}(x) e^{-iH t} = \begin{cases} h_j^{\text{in}}(x+t) & x+t > 0 \\ h_{j+1}^{\text{out}}(-(x+t)) & x+t < 0 \end{cases} \quad (7)$$

The average in (1) can be written in terms of  $H$  and  $\rho_0$  as follows:

$$\langle \dots \rangle_{R, t_0} = \text{Tr} \left( e^{-iH t_0} \rho_0 e^{iH t_0} \dots \right).$$

Further, the steady state (1) is invariant under the  $H$ -evolution, as we will show.

It is clear that in the initial density matrix  $\rho_0$ , the system decouples into its subsystems with Hamiltonians  $H_0^{(j)}$ ,  $j = 1, \dots, N$  on the various legs of the graph. For instance,

$$\left\langle \prod_{j=1}^N h_j^{\text{in}}(x_j) h_j^{\text{out}}(y_j) \right\rangle_{R, 0} = \prod_{j=1}^N \langle h_j^{\text{in}}(x_j) h_j^{\text{out}}(y_j) \rangle_{R, 0}.$$

In the steady state limit, it turns out that the system again decouples, but not into the separate legs of the graph. It rather decouples into  $N$  subsystems, for  $j = 1, \dots, N$ , where in each subsystem  $h_j^{\text{in}}$  and  $h_{j+1}^{\text{out}}$  are coupled to each other, in particular satisfying the first equation of (3).

Let us now construct explicitly the steady state from (1) using the above considerations, and see explicitly the  $H$ -invariance and the decoupling mentioned. This follows the methods of [8, 9]. Assuming that  $R \gg t_0 \gg x > 0$ , we have

$$e^{iH t_0} h_j^{\text{in}}(x) e^{-iH t_0} = h_j^{\text{in}}(x+t_0) \quad (8)$$

$$e^{iH t_0} h_j^{\text{out}}(x) e^{-iH t_0} = h_{j-1}^{\text{in}}(-x+t_0). \quad (9)$$

Evolving the result backward with  $H_0$  then gives

$$e^{-iH_0 t_0} e^{iH t_0} h_j^{\text{in}}(x) e^{-iH t_0} e^{iH_0 t_0} = h_j^{\text{in}}(x) \quad (10)$$

$$e^{-iH_0 t_0} e^{iH t_0} h_j^{\text{out}}(x) e^{-iH t_0} e^{iH_0 t_0} = h_{j-1}^{\text{out}}(x). \quad (11)$$

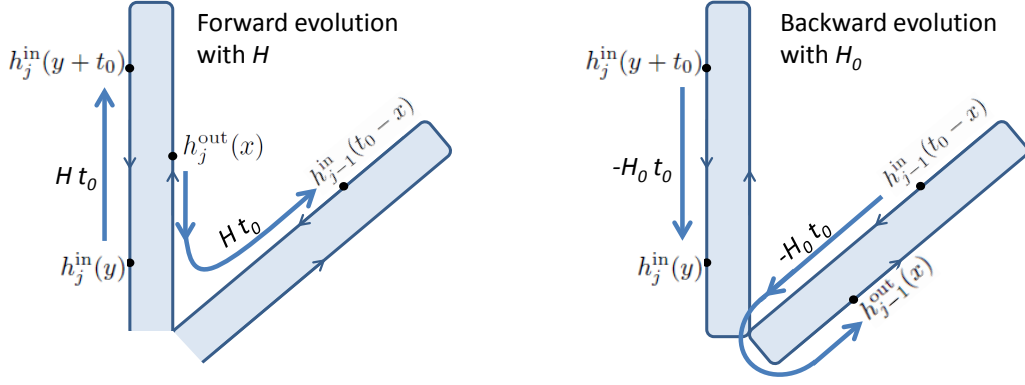


Figure 1: The forward time evolution with  $H$  and subsequent backward time evolution with  $H_0$  of  $h_j^{\text{in}}(y)$  in equation (10) and  $h_j^{\text{out}}(x)$  in equation (11) is shown, focusing only on the  $j$ -th and  $j - 1$ -th legs of the star graph. This shows that measuring  $h_j^{\text{in}}$  and  $h_j^{\text{out}}$  in the steady state corresponds to measuring  $h_j^{\text{in}}$  and  $h_{j-1}^{\text{out}}$  in the disconnected system, respectively.

The above process of forward evolution with  $H$  until the time of connection, and subsequent backward evolution with  $H_0$  is visualized in figure 1

For definiteness, let us consider the observable  $\prod_{j=1}^N h_j^{\text{in}}(x_j) h_j^{\text{out}}(y_j)$ . Using the fact that  $\rho_0$  is  $H_0$ -invariant and the above equations, we then obtain

$$\lim_{R \gg t_0 \rightarrow \infty} \langle \prod_{j=1}^N h_j^{\text{in}}(x_j) h_j^{\text{out}}(y_j) \rangle_{R, t_0} = \langle \prod_{j=1}^N h_j^{\text{in}}(x_j) h_{j-1}^{\text{out}}(y_j) \rangle_{\infty, 0}. \quad (12)$$

This expression is factorized, but the factorization is not in terms of legs. In order to find a steady state that reproduces the above relation, let us introduce the Hamiltonians  $H^{(j,j+1)}$ ,  $j = 1, \dots, N$ , which mutually commute and which couple together  $h_j^{\text{in}}$  with  $h_{j+1}^{\text{out}}$  in the same way  $H_0^{(j)}$  couple together  $h_j^{\text{in}}$  with  $h_j^{\text{out}}$ . It is convenient for our later derivations to consider these Hamiltonians, like the Hamiltonians  $H_0^{(j)}$ , with  $R$  finite. This means that with  $H^{(j,j+1)}$  the continuity conditions are

$$h_j^{\text{in}}(0) = h_{j+1}^{\text{out}}(0), \quad h_{j+1}^{\text{out}}(\frac{R}{2}) = h_j^{\text{in}}(\frac{R}{2}), \quad (13)$$

paralleling (2). Then we may define

$$\rho_{\text{stat}} = \mathbf{n} \left[ e^{-\sum_{j=1}^N \beta_j H^{(j,j+1)}} \right]. \quad (14)$$

We see that any average of an operator  $\mathcal{O}$  with the density matrix  $\rho_0$  is equal to the average of a modified operator  $\tilde{\mathcal{O}}$  with the density matrix  $\rho_{\text{stat}}$ , where  $\tilde{\mathcal{O}}$  is obtained by replacing every  $h_j^{\text{out}}$  by  $h_{j+1}^{\text{out}}$ . Hence we see that the density matrix (14) gives rise to the steady state average,

$$\langle \dots \rangle_{\text{stat}} := \lim_{R \rightarrow \infty} \text{Tr} (\rho_{\text{stat}} \dots), \quad (15)$$

as (12) then implies

$$\lim_{R \gg t_0 \rightarrow \infty} \langle \prod_{j=1}^N h_j^{\text{in}}(x_j) h_j^{\text{out}}(y_j) \rangle_{R, t_0} = \langle \prod_{j=1}^N h_j^{\text{in}}(x_j) h_j^{\text{out}}(y_j) \rangle_{\text{stat}} \quad (16)$$

A similar derivation holds for any other finite product of fields. Since the Hamiltonians  $H^{(j,j+1)}$  commute, this shows the factorization mentioned above. The result below of a nonzero energy current then confirms that this is a non-equilibrium steady state.

A picture representing, side by side, the physical situation after connection, and the Hamiltonians  $H^{(j,j+1)}$  used in the construction of the steady-state density matrix, is shown in Figure 2.

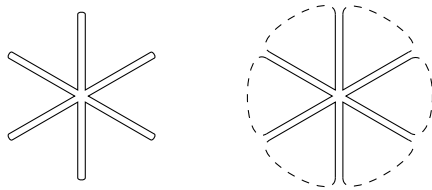


Figure 2: On the left, the physical situation at finite  $R$  after the connection: several heat baths connected at a point. The Hamiltonian  $H$  represents evolution along the path going around the graph. On the right, how expectation values are calculated using the fact that in the steady state limit the system decouples into subsystems as in this picture. The Hamiltonians  $H^{(j,j+1)}$  represent evolutions along the distinct paths. These two time-evolutions are the same for fields near the vertex.

In the  $H^{(j,j+1)}$  subsystems, it is simpler to work with “right-moving” fields only, which are the incoming fields from one leg and the outgoing fields into the next leg. We will label these by the two legs on which they move, and make the following identification:

$$h^{(j,j+1)}(x) := \begin{cases} h_j^{\text{in}}(-x) & x < 0 \\ h_{j+1}^{\text{out}}(x) & x \geq 0 \end{cases}, \quad x \in \left[-\frac{R}{2}, \frac{R}{2}\right]. \quad (17)$$

With these new fields, the time evolution is now simply

$$e^{iHt} h^{(j,j+1)}(x) e^{-iHt} = h^{(j,j+1)}(x - t), \quad x, t \ll R \quad (18)$$

and  $h^{(j,j+1)}(x)$  is continuous.

**Remark 2.1** *It is important to note that the connected-system Hamiltonian  $H$  does not commute with  $H^{(j,j+1)}$ . However, thanks to the agreement between the first equations of (3) and (13), the evolution with  $H$  by a time  $t$  on fields at  $x$ , for any  $R \gg |t|, x > 0$ , is exactly in agreement with the evolution with  $\sum_{j=1}^N H^{(j,j+1)}$ :*

$$H = \sum_{j=1}^N H^{(j,j+1)} \quad \text{as evolution operators on fields a finite distance from the vertex.}$$

*Since  $\sum_{j=1}^N H^{(j,j+1)}$  commutes with  $\rho_{\text{stat}}$ , this implies that the steady state average  $\langle \dots \rangle_{\text{stat}}$  (defined only for products of local fields a finite distance from the vertex) is  $H$ -invariant, as claimed above.*

### 3 Results and discussion

We now state our main results concerning the energy current and its fluctuations in the steady state described in the previous section.

Consider a charge

$$Q = \sum_{j=1}^N \alpha_j H_0^{(j)},$$

the weighted sum of the energies in the various legs of the star graph. The time derivative of  $Q$  is the associated “energy current” operator,  $\mathcal{J} := i[H, Q] = \sum_{j=1}^N \alpha_j (h_j^{\text{out}}(0) - h_j^{\text{in}}(0))$ , which is the weighted sum of the momentum densities on the various legs of the graph. It is local, hence it has a well-defined steady-state average  $J = \langle \mathcal{J} \rangle_{\text{stat}} = i \langle [H, Q] \rangle_{\text{stat}}$ . Note that this steady-state average does not necessarily vanish because  $Q$  itself is not a local operator.

### 3.1 Average current

The average current is in fact simple to evaluate using standard CFT techniques (see for instance [34]) which give the result  $\langle h^{(j,j+1)} \rangle_{\text{stat}} = \pi c / (12\beta_j^2)$ . Hence:

$$J = \frac{\pi c}{12} \sum_{j=1}^N \frac{\Delta\alpha_j}{\beta_j^2} \quad (19)$$

where  $\Delta\alpha_j := \alpha_{j+1} - \alpha_j$ . This generalizes the result of [8], where the case  $N = 2$  and  $\alpha_1 = -\alpha_2 = 1/2$  was considered. This is in agreement with the simple picture according to which energy flows from leg  $j$  to leg  $j + 1$  with the information of the asymptotic thermal bath of leg  $j$ , with a current  $\pi c / (12\beta_j^2)$ .

The charge and energy current has been calculated via a scattering state approach in [27, 29] in the context of free fermion and Luttinger liquid models for more general continuity conditions at the vertex, where the systems also have a set of chemical potentials. As an example, for a system of Dirac fermions (with central charge  $c = 1$ ) the energy current from one leg into the vertex (hence into all other legs) was calculated. Our result agrees with the result found in [27, 29] for a critical system with our sequential boundary conditions and all the chemical potentials set to zero. For more details, see Appendix A.

### 3.2 Current fluctuations

The energy current fluctuations can also be evaluated within our framework. There are various ways of defining these fluctuations. We will consider the setup [7] where the charge  $Q$  is first quantum-mechanically measured (von Neumann measurement) at the contact time  $-t_0$ , and then measured at time 0. The cumulants of the difference  $\Delta_{t_0}Q$  of the measured values are then evaluated in the steady state limit (where in particular  $t_0$  becomes infinite). We find that all cumulants diverge linearly in  $t_0$ , and we obtain the exact coefficients of this divergence for all cumulants. These can be organized into the coefficients of the Taylor expansion in  $i\lambda$  of the scaled cumulant-generating function  $F(\lambda)$ , which is the Legendre transform of the large deviation function. As was shown in [9] (this was the case for  $N = 2$ , but the proof is easily generalizable to all  $N$ ), the result of these operations can be represented by the formula

$$F(\lambda) = \lim_{t \rightarrow \infty} \frac{1}{t} \log \langle e^{i\lambda Q(t)} e^{-i\lambda Q} \rangle_{\text{stat}} \quad (20)$$

where  $Q(t) = e^{iHt} Q e^{-iHt}$ . This is of the same form as the standard expression for the so-called full-counting statistics of charge transfer, which was first obtained within the context of indirect measurements, instead of the two-time von Neuman measurement protocol we discuss above, in free fermion models in [32]. In fact, we will show that formula (20) is equivalent to the simpler, “naive” expression

$$F(\lambda) = \lim_{t \rightarrow \infty} \frac{1}{t} \log \langle e^{i\lambda(Q(t) - Q)} \rangle_{\text{stat}}. \quad (21)$$

This, for instance, immediately implies that the second order in  $i\lambda$ , which is the noise (made up of the thermal noise and the so-called shot noise), takes the familiar form:

$$F(\lambda) = i\lambda J + \frac{(i\lambda)^2}{2} \int_0^\infty dt \left( \langle \{ \mathcal{J}(t), \mathcal{J}(0) \} \rangle_{\text{stat}} - 2J^2 \right) + \dots \quad (22)$$

Further, using the time evolution equations of the previous section, one finds that

$$\Delta_t Q := Q(t) - Q = \sum_j \Delta\alpha_j \int_0^t dx h_j^{\text{in}}(x). \quad (23)$$

Hence, the function  $F(\lambda)$  can also be interpreted as the generating function for large- $L$  cumulants of the weighted sum, over the legs of the graph, of the incoming energies  $\int_0^L dx h_j^{\text{in}}(x)$  on intervals

of lengths  $L$ . In contrast with the initial two-measurement description, in this interpretation, these incoming energies are now measured in single von Neumann measurements.

We find the following exact expression for  $F(\lambda)$ :

$$F(\lambda) = \frac{i\lambda\pi c}{12} \sum_{j=1}^N \frac{\Delta\alpha_j}{\beta_j(\beta_j - i\Delta\alpha_j\lambda)}, \quad (24)$$

generalizing the result of [8] to higher  $N$  and to different charges  $Q$  (different weighted sums). Specializing to the case where the charge measured is the energy difference between two contiguous parts of the star graph  $Q = \frac{1}{2}(H_{\text{part 1}} - H_{\text{part 2}})$ , the cumulant generating function simplifies to:

$$F(\lambda) = \frac{i\lambda\pi c}{12} \left( \frac{1}{\beta_m(\beta_m - i\lambda)} - \frac{1}{\beta_n(\beta_n + i\lambda)} \right) \quad (25)$$

where  $m$  and  $n$  are the legs just after which the sign of the weight changes from minus to plus and from plus to minus, respectively. This result is identical in form to the case  $N = 2$ .

### 3.3 Fluctuation relations and Poisson processes

The function (25) satisfies the usual symmetry relation (or fluctuation relation) found in bipartite systems,

$$F(i(\beta_n - \beta_m) - \lambda) = F(\lambda). \quad (26)$$

This is a standard relation in the context of non-equilibrium steady states, and is characteristic of an exponentially decaying ratio of probabilities for energy transfer from the lower-temperature (larger  $\beta$ ) region and energy transfer from the higher-temperature (smaller  $\beta$ ) region [7], over large periods of time. That is, let  $P_{(2 \text{ parts})}(q)$  be the probability that  $\Delta_{t_0}Q = q$  for this particular choice of weights  $\alpha_j$ . Then (26) is equivalent to a so-called *steady-state* fluctuation theorem:

$$P_{(2 \text{ parts})}(q) \sim e^{(\beta_n - \beta_m)q} P_{(2 \text{ parts})}(-q) \quad (27)$$

where “ $\sim$ ” indicates that the fluctuation relation holds only at large  $t_0$  and accordingly large  $q$ .

In general, however, the cumulant generating function (24) does not satisfy such a simple symmetry relation involving a shift in  $\lambda$  only. Yet there is a simple physical picture behind formula (24), and a generalized symmetry relation that agrees with this picture. Denoting  $\omega_j := \lambda\Delta\alpha_j$ , with  $j = 1, \dots, N$ , the symmetry relation is:

$$F(\omega_1 - i\beta_1, \dots, \omega_N - i\beta_N) \text{ is symmetric under permutations of } \omega_1, \dots, \omega_N. \quad (28)$$

Indeed, we observe that our exact formula (24) satisfies (28):

$$F(\omega_1 - i\beta_1, \dots, \omega_N - i\beta_N) = -\frac{\pi c}{12} \sum_j \left( \frac{1}{\beta_j} + \frac{1}{i\omega_j} \right). \quad (29)$$

The physical picture is as follows. Due to the separation of the stationary state into the  $H^{(j,j+1)}$  subsystems, we expect  $F(\lambda)$  in general to correspond to a set of  $N$  independent processes whereby energy is transferred from leg  $j$  to leg  $j+1$ , with  $j = 1, \dots, N$ . Let  $P^{(j,j+1)}(r)$  be the probability that an energy  $r > 0$  be transferred from leg  $j$  to leg  $j+1$  in such a process (this energy is always positive thanks to our choice of continuity conditions at the vertex). Further, let us denote by  $P_{\Delta\alpha_1, \dots, \Delta\alpha_N}(q)$  the probability that  $\Delta_{t_0}Q = q$  for general weights  $\alpha_j$  (it only depends on the weight differences  $\Delta\alpha_j$ ). We have in particular  $e^{t_0 F(\lambda)} = \int dq e^{i\lambda q} P_{\Delta\alpha_1, \dots, \Delta\alpha_N}(q)$ . Then we expect that at large  $t_0$ , we have

$$P_{\Delta\alpha_1, \dots, \Delta\alpha_N}(q) \sim \int_{q=\sum_j \Delta\alpha_j r_j} \prod_j dr_j P^{(j,j+1)}(r_j). \quad (30)$$



Furthermore, we expect the independent  $j \rightarrow j + 1$  processes to be related to each other via a similar fluctuation relation as (27):

$$e^{\beta_j r} P^{(j,j+1)}(r) \sim e^{\beta_k r} P^{(k,k+1)}(r) \quad \forall \quad j, k. \quad (31)$$

We can verify that in the 2-part case discussed above, we do recover (27):

$$\begin{aligned} e^{\beta_m q} P_{(2 \text{ parts})}(q) &\sim \int_{q=r_m-r_n} dr_m dr_n e^{\beta_m(r_m-r_n)} P^{(m,m+1)}(r_m) P^{(n,n+1)}(r_n) \\ &\sim \int_{q=r_m-r_n} dr_m dr_n e^{\beta_n(r_m-r_n)} P^{(n,n+1)}(r_m) P^{(m,m+1)}(r_n) \\ &= \int_{-q=r_m-r_n} dr_m dr_n e^{\beta_n(r_n-r_m)} P^{(n,n+1)}(r_n) P^{(m,m+1)}(r_m) \\ &\sim e^{\beta_n q} P_{(2 \text{ parts})}(-q). \end{aligned}$$

What's more, this picture implies the generalized symmetry relation (28) for  $F(\lambda)$ . This is simple to see from

$$e^{t_0 F(\omega_1, \dots, \omega_N)} \sim \int \prod_j dr_j e^{i\omega_j r_j} P^{(j,j+1)}(r_j) \quad (32)$$

and using (31).

Hence, our result for the large-time cumulant generating function is indeed in agreement with the proposed picture.

Consider the conditions that (i)  $F(\lambda)$  separates into a sum over  $j$  of a two-variable function of  $\omega_j := \lambda \Delta \alpha_j$  and  $\beta_j$ ; (ii)  $F(\lambda)$  is a homogeneous function of  $\omega_j$  and  $\beta_j$  of degree -1; (iii)  $F(0) = 0$ ; and (iv) the symmetry relation (28) holds. We observe that these conditions are sufficient to fully fix the function  $F(\lambda)$  to the form (24), up to an overall normalization. Indeed, the first condition says that  $F(\lambda) = \sum_j f(\omega_j, \beta_j)$ . Let us denote  $\tilde{f}(\omega, \beta) = f(\omega - i\beta, \beta)$ . Then the fourth condition implies that  $\tilde{f}(\omega, \beta) = \tilde{f}_1(\omega) + \tilde{f}_2(\beta)$ . By the second condition, we then have  $\tilde{f}_1(\omega) = a_1/(i\omega)$  and  $\tilde{f}_2(\beta) = a_2/\beta$ . Further, the third condition says that  $\tilde{f}(i\beta, \beta) = 0$ , which gives  $a_1 = a_2$ . Hence we indeed find the right-hand side of (29) for  $\sum_j f_j(\omega_j, \beta_j)$  up to a normalization, which completes the proof. Condition (i) is a consequence of the factorization of the stationary density matrix (14) and of (23) and (22). Condition (ii) is a consequence of scale invariance, and condition (iii) of the basic definition of the generating function. Hence, along with basic properties of CFT, the symmetry relation (28) fully fixes the cumulant generating function  $F(\lambda)$ . This generalizes what was observed in [8] in the case  $N = 2$ .

We finally note that the independent processes of energy transfer from legs  $j$  and  $j + 1$ , with probabilities  $P^{(j,j+1)}(q)$ , in the asymptotic regime  $t_0 \rightarrow \infty$ , can be uniquely identified. Indeed, we can interpret  $F(\lambda)$  as describing the cumulants of a random variable  $q$  coming from classical processes as follows: at each interface  $j \rightarrow j + 1$ , there is a family of independent Poisson processes parametrized by  $r > 0$ , with intensities  $e^{-\beta_j r}$ , each contributing to the random variable  $q$  a value  $\Delta \alpha_j r$ . This is again a generalization of what was observed in [8] in the case  $N = 2$ , and further confirms that for large energy transfers, CFT is equivalently described by replacing right-movers and left-movers by independent carriers of energy units, distributed according to the appropriate density of state, jumping towards the right and left, respectively, in a Poissonian fashion.

## 4 The continuous Virasoro algebra and its diagrams

Our strategy to prove the form (24) of the cumulant generating function will be an analysis of (20) as a series expansion in  $i\lambda$ , along with the use of the Virasoro algebra at the basis of CFT. This algebraic analysis provides an alternative to the local-variable analysis used in [9] in order to prove (24) in the case  $N = 2$  (and for  $\alpha_1 = -\alpha_2 = 1/2$ ). The Virasoro algebra occurs as a natural algebra

in the quantization of CFT on the circle or on segments (or in radial quantization). Of course, in the construction discussed in Section 2, we have instead, after the connection, the star-graph geometry; yet the usual notions of CFT on segments of lengths  $R/2$  can still be used.

A complete analysis of the quench using the standard formulation of the Virasoro algebra would be interesting. Some initial ideas are presented in Appendix B, where it turns out we obtain the expected value of the holomorphic dimension of the branch point twist field [35], which is used in entanglement entropy.

However, in the establishment of the steady state through the steady-state limit (1), the large- $R$  limit needs to be taken before the time evolution can be analyzed. The large- $R$  limit of the quantization on the circle or on segments gives rise to the quantization on the line or the semiline (depending on how exactly the limit is taken). In this quantization space, the Virasoro algebra is no longer a natural algebra. At equilibrium, one can circumvent this problem, as one knows the Euclidean geometry describing the large- $R$  limit: either a cylinder, infinite or semi-infinite (at finite temperature, with the circumference equal to the inverse temperature), or the plane or half-plane (at zero temperature). In these cases, either using the quantization on the circle or radial quantization, one can still make use of the Virasoro algebra. However, out of equilibrium, there is not yet a clear Euclidean geometric picture; hence one needs to keep the quantization on the line or the semi-line (here, appropriately tailored to the graph geometry), whence one loses the Virasoro algebra.

The natural algebraic structure that emerges in the large- $R$  limit is that which one may refer to as the *continuous Virasoro algebra*. This is an algebra similar to the Virasoro algebra, but with a continuous index. The algebraic structure is rather simple, but its connection to the result of the large- $R$  limit of the Virasoro algebra present some subtleties. Its representation theory also presents many subtleties, which we will not address here. We present instead basic aspects of this algebra and the diagrams used to evaluate certain traces of product of algebra elements, which we will need in the next section.

## 4.1 Definitions

Consider a Lie algebra with a continuous basis

$$\{a_p : p \in \mathbb{R}\} \quad (33)$$

satisfying the following commutation relations

$$[a_p, a_q] = (p - q)a_{p+q} + (2pk + \frac{c}{12}p^3)\delta(p + q) \quad (34)$$

where<sup>3</sup>  $k, c \in \mathbb{R}$ . For a fixed  $c$ , the algebras corresponding to different values of  $k$  are isomorphic: a simple change of basis  $\tilde{a}_p = a_p + k\delta(p)$  makes the linear-in- $p$  term vanish. However it is convenient for us to keep this term. Given an appropriate highest-weight representation of this algebra, where  $a_0$  is diagonalizable and with eigenvalues that are bounded from below, we may define a state by the following ratio of traces

$$\langle \dots \rangle_\beta \equiv \frac{\text{Tr}(e^{-2\pi\beta a_0} \dots)}{\text{Tr}(e^{-2\pi\beta a_0})} \quad (35)$$

where  $\dots$  represents some product of the generators  $a_p$ , and  $\beta > 0$  is some parameter. A simple calculation using (34), and assuming that the cyclic property of the trace holds,

$$\langle a_p \rangle_\beta = \frac{\text{Tr}(e^{-2\pi\beta a_0} a_p)}{\text{Tr}(e^{-2\pi\beta a_0})} = \frac{\text{Tr}(a_p e^{-2\pi\beta a_0})}{\text{Tr}(e^{-2\pi\beta a_0})} = e^{-2\pi\beta p} \langle a_p \rangle_\beta = 0 \quad \text{for } p \neq 0,$$

shows that we must have

$$\langle a_p \rangle_\beta = B \delta(p) \quad (36)$$

---

<sup>3</sup>Instead of seeing  $k, c$  as numbers, we could also see them as additional central elements; but in the representation we will need these simply take fixed values.

for some number  $B$ . With an appropriate choice of basis, it is possible to impose

$$B = 0.$$

With this condition, the basis is completely fixed (albeit in a state-dependent way) and in particular  $k$  in (34) is unambiguous. Below we will have a representation where with the condition  $B = 0$ ,

$$k = k(\beta) := \frac{c}{24\beta^2}. \quad (37)$$

We can then calculate expectation values of products of more than one generator, again using the cyclic property of the trace along with the algebra relations. For example,

$$\begin{aligned} \langle a_{p_1} a_{p_2} \rangle_\beta &= \frac{\text{Tr}(e^{-2\pi\beta a_0} a_{p_1} a_{p_2})}{\text{Tr}(e^{-2\pi\beta a_0})} = \frac{\text{Tr}(a_{p_2} e^{-2\pi\beta a_0} a_{p_1})}{\text{Tr}(e^{-2\pi\beta a_0})} = e^{-2\pi\beta p_2} \langle a_{p_2} a_{p_1} \rangle_\beta = \frac{1}{e^{2\pi\beta p_2} - 1} \langle [a_{p_2}, a_{p_1}] \rangle_\beta \\ &= \frac{1}{e^{2\pi\beta p_2} - 1} \left( 2p_2 k(\beta) + \frac{c}{12} p_2^3 \right) \delta(p_1 + p_2). \end{aligned} \quad (38)$$

## 4.2 Diagrams

Expectation values of products of several generators  $a_p$  can be calculated similarly using the cyclic property of traces on, for instance, the rightmost generator, giving

$$\langle a_{p_1} \cdots a_{p_M} \rangle_\beta = \frac{1}{e^{2\pi\beta p_M} - 1} \sum_{j=1}^{M-1} \langle a_{p_1} \cdots [a_{p_M}, a_{p_j}] \cdots a_{p_{M-1}} \rangle_\beta. \quad (39)$$

One obtains a recursion relation for these expectation values by using (34) for the commutator. There are two terms occurring: the first is proportional to the generator  $a_{p_j+p_M}$ , and the second is the central term, with a delta function factor  $\delta(p_j + p_M)$ . We may represent these two contributions using the following diagrams:

$$\begin{array}{c} \bullet \\ | \\ \bullet \end{array} \begin{array}{c} p_1 + p_2 \\ \text{---} \\ \bullet \end{array} \begin{array}{c} \bullet \\ | \\ \bullet \end{array} \begin{array}{c} p_2 \\ \text{---} \\ \bullet \end{array} = \frac{p_2 - p_1}{e^{2\pi\beta p_2} - 1} \quad (40a)$$

$$\begin{array}{c} \bullet \end{array} \begin{array}{c} \text{---} \\ \bullet \end{array} \begin{array}{c} \bullet \\ \text{---} \\ \bullet \end{array} \begin{array}{c} p_2 \\ \text{---} \\ \bullet \end{array} = \frac{1}{e^{2\pi\beta p_2} - 1} \left( 2p_2 k(\beta) + \frac{c}{12} p_2^3 \right) \delta(p_1 + p_2). \quad (40b)$$

Repeating the process, we obtain the expectation value as a sum of diagrams constructed according to the following rules:

1. Start with a horizontal alignment of “open dots” carrying momenta  $p_1, \dots, p_M$ , for instance

$$\begin{array}{ccccccccc} \bullet & & \bullet & & \bullet & & \bullet & & \bullet \\ p_1 & & p_2 & & p_3 & & p_4 & & p_5 \end{array}$$

2. Connect the rightmost dot with a dot to its left, using either the vertex (40a) or the cap (40b). The use of the vertex (40a) leaves an open dot at the horizontal position of the leftmost dot in the connected pair, and at one vertical step higher, carrying the sum of momenta of the connected dots. The use of the cap (40b) closes both dots connected. If there are only two open dots, use only (40b).
3. Repeat the previous step with the remaining open dots, one vertical step higher.
4. Finish when there are no remaining open dots.

Note that we do not allow for diagrams with a single open dot; this corresponds to our choice of basis according to which  $\langle a_p \rangle = 0$ . As an example, two diagrams contributing to the expectation value  $\langle a_{p_1} a_{p_2} a_{p_3} a_{p_4} a_{p_5} \rangle_\beta$  are



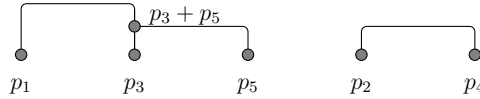
The first diagram corresponds to the term

$$\frac{p_5 - p_2}{e^{2\pi\beta p_5} - 1} \frac{p_4 - p_3}{e^{2\pi\beta p_4} - 1} \frac{p_3 + p_4 - (p_2 + p_5)}{e^{2\pi\beta(p_3+p_4)} - 1} \times \frac{2(p_2 + p_3 + p_4 + p_5)k(\beta) + \frac{c}{12}(p_2 + p_3 + p_4 + p_5)^3}{e^{2\pi\beta(p_2+p_3+p_4+p_5)} - 1} \delta(p_1 + p_2 + p_3 + p_4 + p_5), \quad (41)$$

and the second diagram corresponds to the term

$$\frac{p_5 - p_3}{e^{2\pi\beta p_5} - 1} \frac{2(p_3 + p_5)k(\beta) + \frac{c}{12}(p_3 + p_5)^3}{e^{2\pi\beta(p_3+p_5)} - 1} \delta(p_1 + p_3 + p_5) \frac{2p_4 k(\beta) + \frac{c}{12}p_4^3}{e^{2\pi\beta p_4} - 1} \delta(p_2 + p_4). \quad (42)$$

Note that the second diagram can be written as a product of two separate diagrams



We will call a diagram “connected” if there is a connected path between all initial dots; otherwise it is “disconnected”. Above, the first diagram is connected, while the second is disconnected. It is clear, from our diagrammatic rules, that a disconnected diagram can always be written as a product of connected diagrams. Note also that the value of the momentum is conserved at each three-leg vertex introduced by the first type of connection (40a), and that the second type of connection (40b) produces a factor of a delta function that sets the sum of the momenta to zero. Hence, the set of momenta in every connected diagram is constrained to sum to zero, but has no other constraint.

As another example, the full expression for the expectation value  $\langle a_{p_1} a_{p_2} a_{p_3} a_{p_4} \rangle_\beta$  is

We finally note that diagrams obtained according to the above rules have a nice dynamic interpretation. Indeed, we imagine starting with  $N$  particles, carrying conserved quantities  $p_j$ , which can only move left, such that two particles can either jump through each other without interacting, or interact with each other by forming a bound state (a new particle) or by annihilating each other. Observing diagrams from bottom to top and interpreting them as world-lines, with time increasing upwards, the rules above give rise to all possible inequivalent events for this dynamics with the further constraint that the right-most particle always interact first.

### 4.3 A combinatoric formula

We now show that our rules for constructing diagrams imply that every expectation value can be written as a sum over all partitions of the initial set of momenta, where each term in the sum is the product over all subsets forming the partition, of the sum of all connected diagrams associated to the subset. That is, let  $P = (p_1, \dots, p_M)$  be a list of momenta, and for any ordered sublist  $s \subset P$  (i.e. any sublist  $(p_{j_1}, \dots, p_{j_m})$  with  $j_1 < \dots < j_m$ ), let us denote by  $C(s)$  the sum of all diagrams associated to  $s$  constructed according to the rules above and which are connected. Then we show that

$$\langle a_{p_1} \cdots a_{p_M} \rangle_\beta = \sum_S C(s_1) \cdots C(s_n) \quad (44)$$

where the sum is over the partitions  $S = \{s_1, \dots, s_n\}$  of  $P$ :

$$s_1 \subset P, \dots, s_n \subset P, \quad \bigcup_i s_i = P, \quad s_i \cap s_j = \emptyset \quad (i \neq j). \quad (45)$$

Let us call “admissible” a diagram based on a list  $s$  of momenta, which satisfies our rules for diagram construction. Let us denote by  $D_P$  the set of all admissible diagrams based on  $P$ , by  $D_s^C$  the set of all admissible connected diagrams based on the ordered sublist  $s$  of  $P$ , and by  $\tilde{D}_P = \cup_S D_{s_1}^C \cdots D_{s_n}^C$  the set of all products (juxtapositions) of connected admissible diagrams based on all partitions  $S$  of  $P$ . In order to show (44), we only need to show  $D_P = \tilde{D}_P$ . The proof is in three steps. First, we show that the connected factors in every admissible diagram are themselves admissible diagrams, based on the list of momenta which they connect. Second, we show that every admissible diagram based on  $P$  is a product of connected factors based on a partition  $S$  of  $P$ . These first two points show that  $D_P \subset \tilde{D}_P$ . Last, we show that every product of connected admissible diagrams based on a partition  $S$  of  $P$  is an admissible diagram based on  $P$ . This shows  $\tilde{D}_P \subset D_P$ , proving the equality.

Given a pair of dots that are connected either with (40a) or with (40b), we will refer to its horizontal position as the horizontal position of the rightmost member of the pair, and to its vertical position as the height of the flat horizontal part of the diagram component (40a) or (40b). Then, we remark the following.

**Remark 4.1** *The set of all diagrams formed using our rules is the set of all diagrams obtained from the basic components (40a) and (40b), under the unique additional condition that the bottom-to-top ordering of the vertical positions of the connections be in agreement with the right-to-left ordering of their horizontal position.*

Indeed, it is clear that the rules provide diagrams that satisfy the additional condition of this remark. Further, given a diagram that does satisfy it, we may scan the rightmost members of the connected pairs from the right to the left; we observe that under such a scan the connections exactly agree with the rules.

For the first step of the proof of (44), let us consider a connected factor, and the initial dots that are being connected within the factor. These correspond to an ordered sublist  $s$  of the initial list  $P$ , and are horizontally aligned and ordered. Then, according to Remark 4.1, the bottom-to-top ordering of the connections within the factor are in agreement with the right-to-left ordering of the right-members of the connected pairs within the factor; again according to Remark 4.1, this implies that a connected factor is an admissible diagram.

The second step is simply a consequence of the fact that given an admissible diagram, the relation according to which two elements of  $P$  belong to the same connected factor is an equivalence relation.

The last step is based on the simple observation that within a connected admissible diagram, it is always possible to move the connections vertically so as to space them out, keeping their order the same. Consider a partition  $S$  of  $P$  and a product of connected admissible diagrams based on  $S$ . Let us draw the product of diagrams with the original dots corresponding to  $P$  in ordered horizontal alignment. Let us scan the rightmost members of the connected pairs in the full diagram from the

right to the left. Going through connected pairs in a connected factor we observe the correct vertical ordering of the connections. As we go from a pair in a connected factor to a new pair in a new connected factor, we impose the correct vertical ordering by moving up all connections of the new connected factor at or above the level of the new pair. This does not affect connections in other connected factors. At the end of this process, the additional condition of Remark 4.1 is satisfied for the full diagram, hence the diagram is admissible.

## 5 Full Counting Statistics

In this section we calculate the full counting statistics (20), proving Formula (24). First, we show that the large  $R$  limit of the average in the formula (20) can be calculated using the continuous Virasoro algebra introduced in the previous section. With that, it is clear that after taking the logarithm, only the connected diagrams survive thanks to (44). Then, we show that in the large  $t$  limit, these connected diagrams have a simple dependence on the number of generators, and resumming the orders of  $\lambda$ , we end up with the desired expression (24).

### 5.1 Full counting statistics in terms of Virasoro algebra

As explained in Section 2, in the steady state limit, the system factorises into subsystems described by the Hamiltonians  $H^{(j,j+1)}$ , so that expectation values for local fields can be calculated using the steady state density matrix (14), see Figure 2. By rewriting the product of exponentials in (20) as

$$e^{i\lambda Q(t)} e^{-i\lambda Q} = e^{i\lambda Q + i\lambda \Delta_t Q} e^{-i\lambda Q} = \mathcal{P} \exp \left( i \int_0^\lambda d\lambda' \Delta_t Q(\lambda') \right), \quad (46)$$

we see that we need to evaluate steady-state averages of  $\Delta_t Q = Q(t) - Q$  evolved with  $Q$ :

$$\Delta_t Q(\lambda') := e^{i\lambda' Q} \Delta_t Q e^{-i\lambda' Q}, \quad (47)$$

and ordered products thereof. The quantity  $\Delta_t Q$  was shown in (23) to depend only on the incoming fields  $h_j^{\text{in}}$ , for  $j = 1, \dots, N$ . Using (17), we can replace these with the chiral fields  $h^{(j,j+1)}$ , and write:

$$\Delta_t Q = \sum_{j=1}^N \Delta \alpha_j \int_0^t dx h^{(j,j+1)}(-x). \quad (48)$$

Recall that  $i[H_0^j, h_j^{\text{in}}(x)] = \delta_{j,j'} \partial_x h_j^{\text{in}}(x)$ . Since also  $i[H^{(j,j+1)}, h^{(j',j'+1)}(-x)] = \delta_{j,j'} \partial_x (h^{(j',j'+1)}(-x))$ , the action of  $Q = \sum_j \alpha_j H_0^j$  on  $\Delta_t Q$  is the same as the action of  $\sum_j \alpha_j H^{(j,j+1)}$ . Therefore, in (47), we can make the following replacement:

$$Q \mapsto \sum_{j=1}^N \alpha_j H^{(j,j+1)}.$$

Hence, the  $Q$ -evolution of “time”  $\lambda$  is the same as a  $H$ -evolution where fields are evolved over a time  $\lambda \alpha_j$ , which depends on the leg the fields are on. The above results mean that the path-ordered exponential in (46) actually *factorizes* amongst the subsystems  $H^{(j,j+1)}$ , as does the stationary density matrix (14). Hence the average in (20) is a sum of terms of similar form. In order to evaluate these terms, we need to introduce the appropriate algebraic setup.

The expression (46) is plagued by UV divergencies coming from local operators  $h^{(j,j+1)}(x)$  at coinciding positions. We will use an explicit regularization below.

As is well known (see for instance the book [34]), the algebraic setup underlying CFT is based on the Virasoro algebra. This means that we can calculate the expectation value in (20) using  $N$  commuting copies of a Virasoro algebra,  $L_n^{(j,j+1)}$ ,  $n \in \mathbb{Z}$ ,  $j = 1, \dots, N$ :

$$[L_m^{(j,j+1)}, L_n^{(j,j+1)}] = (m - n) L_{m+n}^{(j,j+1)} + \frac{c}{12} (n^3 - n) \delta_{m+n,0}. \quad (49)$$

There is one copy for the chiral fields in each subsystem  $(j, j + 1)$ , living on the line segment  $[-\frac{R}{2}, \frac{R}{2}]$  with the endpoints identified (see Figure 2). In terms of this algebra, the energy density operator and the Hamiltonian are given by

$$h^{(j,j+1)}(x) = \frac{2\pi}{R^2} \left( \sum_{n=-\mathcal{N}}^{\mathcal{N}} L_n^{(j,j+1)} e^{2\pi i n x / R} - \frac{c}{24} \right), \quad H^{(j,j+1)} = \frac{2\pi}{R} \left( L_0^{(j,j+1)} - \frac{c}{24} \right), \quad (50)$$

and the steady state density matrix takes the following form:

$$\rho_{\text{stat}} = \lim_{R \rightarrow \infty} \mathbf{n} \left[ e^{-\sum_j \beta_j \frac{2\pi}{R} L_0^{(j,j+1)}} \right]. \quad (51)$$

In (50) we have used an explicit UV regularization by summing over a finite number of modes  $L_n^{(j,j+1)}$ . This is equivalent to smearing out the local densities  $h^{(j,j+1)}(x)$ .

Note that the constant terms in (50) cancel out and do not play any role in the considerations below. Performing the integral over  $x$ , we have, from (48),

$$\Delta_t Q = \frac{2\pi}{R^2} \sum_{j=1}^{\mathcal{N}} \Delta \alpha_j \sum_{n=-\mathcal{N}}^{\mathcal{N}} L_n^{(j,j+1)} \int_{-t}^0 dx e^{2\pi i n x / R} = \sum_{j=1}^{\mathcal{N}} \Delta \alpha_j \left( \tilde{S}^j + S^j \right), \quad (52)$$

with

$$\tilde{S}^j := \frac{2\pi t}{R^2} L_0^{(j,j+1)}, \quad S^j := \frac{2}{R} \sum_{\substack{n=-\mathcal{N}, \\ n \neq 0}}^{\mathcal{N}} L_n^{(j,j+1)} e^{-i\pi n t / R} \frac{\sin\left(\frac{\pi n t}{R}\right)}{n}. \quad (53)$$

The  $Q$ -evolution in the path-ordered exponential does not affect  $\tilde{S}^j$ , since  $[Q, \tilde{S}^j] = 0$ . However,  $S^j$  is affected by the action of  $Q$ . Using

$$e^{i\lambda' \alpha_j \frac{2\pi}{R} L_0^{(j,j+1)}} L_n^{(j,j+1)} e^{-i\lambda' \alpha_j \frac{2\pi}{R} L_0^{(j,j+1)}} = L_n^{(j,j+1)} e^{-i\lambda' \alpha_j \frac{2\pi}{R} n},$$

we can write the  $Q$ -evolution of a “time”  $\lambda'$  as a shift of the time variable appearing in the exponential in (53) of twice the value  $\lambda' \alpha_j$ , replacing  $S^j$  with  $S_{\lambda' \alpha_j}^j$  where

$$S_{\lambda'}^j := \sum_{\substack{n=-\mathcal{N}, \\ n \neq 0}}^{\mathcal{N}} L_n^{(j,j+1)} e^{-i\pi n(t+2\tau)/R} \frac{\sin\left(\frac{\pi n t}{R}\right)}{n}. \quad (54)$$

Then, the factorized form of the path-ordered exponential in (46) is, after changing variable to  $\tau = \lambda' \alpha_j$  for convenience,

$$\mathcal{P} \exp \left( i \int_0^\lambda d\lambda' \Delta_t Q(\lambda') \right) = \prod_{j=1}^{\mathcal{N}} \mathcal{P} \exp \left( \frac{i \Delta \alpha_j}{\alpha_j} \int_0^{\lambda \alpha_j} d\tau (\tilde{S}^j + S_\tau^j) \right). \quad (55)$$

Taking the log, (20) gives a sum over the legs,

$$F(\lambda) = \sum_{j=1}^{\mathcal{N}} f(\alpha_j, \Delta \alpha_j, \beta_j, \lambda) \quad (56)$$

with

$$f(\alpha, \Delta \alpha, \beta, \lambda) := \lim_{t \rightarrow \infty} \frac{1}{t} \log \lim_{R \rightarrow \infty} \langle \mathcal{P} \exp \left( \frac{i \Delta \alpha}{\alpha} \int_0^{\lambda \alpha} d\tau (\tilde{S} + S_\tau) \right) \rangle_{\beta, R}. \quad (57)$$

Since the form of this expression is identical for each subsystem  $(j, j + 1)$ , we here and below use a single copy of the Virasoro algebra (49), denoted  $L_n$ ,  $n \in \mathbb{Z}$ , and similarly we drop the superscripts

$j$  on  $\tilde{S}$  and  $S$ . Here, the average  $\langle \cdots \rangle_{\beta,R}$  is the trace over a representation of this single copy of the Virasoro algebra, with density matrix  $\mathbf{n}[\exp(-\beta \frac{2\pi}{R} L_0)]$ :

$$\langle \cdots \rangle_{\beta,R} := \text{Tr} \left( \mathbf{n} \left[ e^{-\beta \frac{2\pi}{R} L_0} \right] \cdots \right).$$

Expanding the path-ordered exponential in (57) and taking the average, we get a sum over  $m \geq 0$  of

$$\left( \frac{i\Delta\alpha}{\alpha} \right)^m \int_0^{\lambda\alpha} d\tau_1 \cdots \int_0^{\tau_{m-1}} d\tau_m \langle (\tilde{S} + S_{\tau_1}) \cdots (\tilde{S} + S_{\tau_m}) \rangle_{\beta,R}. \quad (58)$$

In the following we will show that the limit  $R \rightarrow \infty$  of these averages can be calculated using the continuous Virasoro algebra of the previous section, with the value (37) of  $k$ .

## 5.2 Expectation values in the large $R$ limit

We now show that the large  $R$  limit of a product of Virasoro generators can be calculated using the continuous algebra of the previous section. We will proceed by showing first that this is the case for an expectation value of two generators, and then by induction that it holds for any number of generators.

It turns out that in the large  $R$  limit we should take the UV regularization  $\mathcal{N}$  to grow proportionally to  $R$ , thus introducing a fixed energy cutoff  $\Lambda$ , given by  $\mathcal{N} = \Lambda R$ .

In order to make the connection to the continuous algebra clear, we will make use of the following notation,

$$p_i := \frac{n_i}{R}, \quad a_{p_i}^{(R)} := \frac{L_{n_i}}{R} (1 - \delta_{n_i,0}), \quad A^{(R)} := \frac{L_0}{R^2}, \quad \delta^{(R)}(p_i - p_j) := R\delta_{n_i,n_j}, \quad (59)$$

where the label  $(R)$  indicates that these quantities are defined for finite system size  $R$ . Note in particular that according to our definition,  $a_0^{(R)} = 0$ , which is for convenience.

In (58), we see that we need averages of products of  $\tilde{S}$  and  $S_\tau$ . The latter is a sum over  $n \neq 0$ , the former contains  $L_0$  only. Hence, we are interested in evaluating sums over  $n_i \in \mathbb{Z}$  of averages of products of operators  $a_{p_i}^{(R)}$  and operators  $A^{(R)}$  (the condition  $n_i \neq 0$  is already implemented in the definition of  $a_{p_i}^{(R)}$ ). We will evaluate these sums, in the large- $R$  limit, as integrals over continuous momenta  $p_i$  of averages of operators  $a_{p_i}$  in the continuous Virasoro algebra developed in the previous section. More precisely, we will show that the following is true, for every  $M \geq 0$ , every  $\ell \geq 0$  and every continuous function  $f$  of the momenta (on the left-hand side,  $p_i = n_i/R$  with  $n_i \in \mathbb{Z}$ ; on the right-hand side,  $p_i \in \mathbb{R}$ ; we use the notation  $\mathbf{p} = (p_1, \dots, p_M)$ ):

$$\lim_{R \rightarrow \infty} \sum_{\mathbf{p}=-\Lambda}^{\Lambda} f(\mathbf{p}) \langle a_{p_1}^{(R)} \cdots a_{p_M}^{(R)} \rangle_{\beta,R} = \int_{-\Lambda}^{\Lambda} d^M p f(\mathbf{p}) \langle a_{p_1} \cdots a_{p_M} \rangle_{\beta} \quad (60a)$$

$$\lim_{R \rightarrow \infty} \sum_{\mathbf{p}=-\Lambda}^{\Lambda} f(\mathbf{p}) \langle (A^{(R)})^\ell a_{p_1}^{(R)} \cdots a_{p_M}^{(R)} \rangle_{\beta,R} = (k(\beta))^\ell \int_{-\Lambda}^{\Lambda} d^M p f(\mathbf{p}) \langle a_{p_1} \cdots a_{p_M} \rangle_{\beta}, \quad (60b)$$

as well as a similar statements as (60b), with the  $A^{(R)}$  operators in all possible positions in the average on the left-hand side. On the right-hand side of (60), the averages are calculated using the continuous Virasoro algebra of the previous section with  $k = k(\beta)$ . Recall that  $k(\beta)$ , defined in (37), equals  $c/(24\beta^2)$ . This is the expectation value of the operator  $A^{(R)}$  in the large  $R$  limit (see for instance [34]):

$$\lim_{R \rightarrow \infty} \langle A^{(R)} \rangle_{\beta,R} = \frac{c}{24\beta^2}. \quad (61)$$

The statement (62b), and its relative with different positions of  $A^{(R)}$ , can be interpreted by saying that the operator  $A^{(R)}$  tends, in the infinite- $R$  limit, to a central element, which assumes a fixed, state-dependent value.



Defining  $a_p^{(R)}$  as being zero at  $p = 0$  is appropriate because it automatically implements the condition  $n \neq 0$  in the sum defining  $S_\tau$ . Also, we note that the large- $R$  limit of  $L_0/R$  diverges: it is the operator that measures the energy in the system. The quantity proportional to  $L_0$  and that has a finite large  $R$  limit is  $A^{(R)}$ , which corresponds to the energy density.

The induction proof that we present below is an induction on  $M$ . We will assume that

$$\lim_{R \rightarrow \infty} \langle a_{p_1}^{(R)} \cdots a_{p_M}^{(R)} \rangle_{\beta, R} \doteq \langle a_{p_1} \cdots a_{p_M} \rangle_{\beta} \quad (62a)$$

$$\lim_{R \rightarrow \infty} \langle (A^{(R)})^\ell a_{p_1}^{(R)} \cdots a_{p_M}^{(R)} \rangle_{\beta, R} \doteq (k(\beta))^\ell \langle a_{p_1} \cdots a_{p_M} \rangle_{\beta}, \quad (62b)$$

holds for some  $M$  and for all  $\ell \geq 0$  (as well as similar equations as (62b) but with the  $A^{(R)}$  operators in different positions), and show that this implies the same for  $M + 1$ . We will also show that this holds for  $M = 2$ . Here the equations are understood as distributions, in the sense of (60), which we represent by the equality symbol “ $\doteq$ ”. In practice, this means that the limits on the left-hand sides are taken with fixed  $p_i$ , terms giving zero under integration on the right-hand sides are neglected, and the distribution relation

$$\delta^{(R)}(p_i - p_j) \rightarrow \delta(p_i - p_j). \quad (63)$$

is used. The passage from (62) to (60) is then simply done by using the relation

$$\sum_{\substack{n=-\Lambda R, \\ n \neq 0}}^{\Lambda R} \frac{1}{R} \rightarrow \int_{-\Lambda}^{\Lambda} dp.$$

For lightness of notation we will omit the explicit integration boundaries below.

### 5.2.1 Proof at order 2

The left-hand side of (62a) for the case  $M = 2$  can be written in terms of Virasoro generators, using the definitions (59) and assuming for now  $p_1 \neq 0$  and  $p_2 \neq 0$ :

$$\langle a_{p_1}^{(R)} a_{p_2}^{(R)} \rangle_{\beta, R} = \frac{1}{R^2} \langle L_{n_1} L_{n_2} \rangle_{\beta, R} = \frac{1}{R^2} \frac{\text{Tr} \left( e^{-\beta \frac{2\pi}{R} L_0} L_{n_1} L_{n_2} \right)}{\text{Tr} \left( e^{-\beta \frac{2\pi}{R} L_0} \right)}.$$

Making use of the cyclicity of the trace and the Virasoro algebra, in particular the exchange relation

$$L_n e^{-\frac{2\pi\beta}{R} L_0} = e^{-\frac{2\pi\beta}{R} n} e^{-\frac{2\pi\beta}{R} L_0} L_n, \quad (64)$$

the result is

$$\langle L_{n_1} L_{n_2} \rangle_{\beta, R} = \frac{1}{e^{2\pi\beta n_2/R} - 1} \left( (n_2 - n_1) \langle L_{n_1+n_2} \rangle_{\beta, R} + \frac{c}{12} (n_2^3 - n_2) \delta_{n_1+n_2, 0} \right).$$

Because  $\langle L_n \rangle_{\beta, R} = 0$  for  $n \neq 0$ , we can write the average of two generators as

$$\langle L_{n_1} L_{n_2} \rangle_{\beta, R} = \frac{1}{e^{2\pi\beta n_2/R} - 1} \left( 2n_2 \langle L_0 \rangle_{\beta, R} + \frac{c}{12} (n_2^3 - n_2) \right) \delta_{n_1+n_2, 0},$$

which we can express back in terms of the quantities  $A^{(R)}$ ,  $a_p^{(R)}$ ,  $p$  and  $\delta^{(R)}(p)$  using (59):

$$\langle a_{p_1}^{(R)} a_{p_2}^{(R)} \rangle_{\beta, R} = \frac{1}{e^{2\pi\beta p_2} - 1} \left( 2p_2 \langle A^{(R)} \rangle_{\beta, R} + \frac{c}{12} \left( p_2^3 + \frac{p_2}{R^2} \right) \right) \delta^{(R)}(p_1 + p_2). \quad (65)$$

Taking the limit  $R \rightarrow \infty$  and using the delta-function limit (63) and the expectation value of  $A^{(R)}$  (61), we find

$$\lim_{R \rightarrow \infty} \langle a_{p_1}^{(R)} a_{p_2}^{(R)} \rangle_{\beta, R} \doteq \frac{1}{e^{2\pi\beta p_2} - 1} \left( 2p_2 \frac{c}{24\beta^2} + \frac{c}{12} p_2^3 \right) \delta(p_1 + p_2).$$

This is in fact true for general  $p_1$  and  $p_2$ , noting that although for  $p_1 = p_2 = 0$  the left-hand side is zero and the right-hand side is not, the difference does integrate to zero. The right-hand side corresponds to the value one would obtain by evaluating  $\langle a_{p_1} a_{p_2} \rangle_\beta$  using the diagram rules in the previous section for the choice  $k = c/(24\beta^2)$ . This shows (62a) for  $M = 2$ .

Let us now show (62b) for  $M = 2$ . Starting with  $\ell = 1$ , we can write the insertion of  $A^{(R)}$  in terms of the Virasoro generators as

$$\langle A^{(R)} a_{p_1}^{(R)} a_{p_2}^{(R)} \rangle_{\beta,R} = \frac{1}{R^2} \langle L_0 a_{p_1}^{(R)} a_{p_2}^{(R)} \rangle_{\beta,R}.$$

In general, inserting an extra  $L_0$  in an average of an operator  $\mathcal{O}$  can be done by differentiating with respect to  $\beta$ ,

$$\frac{\partial}{\partial \beta} \langle \mathcal{O} \rangle_{\beta,R} = -\frac{2\pi}{R} \langle L_0 \mathcal{O} \rangle_{\beta,R} + \frac{2\pi}{R} \langle L_0 \rangle \langle \mathcal{O} \rangle_{\beta,R}. \quad (66)$$

Hence, the insertion of  $A^{(R)}$  is equivalent to the application of a differential operator:

$$\langle A^{(R)} \mathcal{O} \rangle_{\beta,R} = \left( \langle A^{(R)} \rangle_{\beta,R} - \frac{1}{2\pi R} \frac{\partial}{\partial \beta} \right) \langle \mathcal{O} \rangle_{\beta,R}. \quad (67)$$

Specializing to the case  $\mathcal{O} = a_{p_1}^{(R)} a_{p_2}^{(R)}$  and looking at (65), one can see that the large  $R$  limit commutes with the  $\partial/\partial\beta$  derivative (in (65), a careful analysis is necessary in order to see this on the average  $\langle A^{(R)} \rangle_{\beta,R}$ , which is beyond the scope of this paper). Hence the last term on the right-hand side above vanishes in the limit, which shows (62b) using (61). Insertions of  $\ell > 1$  operators  $A^{(R)}$  are obtained similarly by multiple applications of the differential operator. Furthermore, the fact that the position of  $A^{(R)}$  is unimportant is an immediate consequence of the commutation relation

$$[a_p^{(R)}, A^{(R)}] = \frac{p}{R} a_p^{(R)} \rightarrow 0 \quad \text{as } R \rightarrow \infty \quad (68)$$

where the large- $R$  limit is taken inside averages and with fixed  $p$ , as above.

### 5.2.2 The induction step

In order to prove that (62a) holds for all values of  $M$ , we must now prove the induction step: if (62a) holds up to some number  $M$  of generators, it must also hold for  $M + 1$  generators.

The finite- $R$  expectation value of  $M + 1$  operators, again assuming all  $p_i$ s different from zero,

$$\langle a_{p_1}^{(R)} \cdots a_{p_{M+1}}^{(R)} \rangle_{\beta,R} = \frac{1}{R^{M+1}} \langle L_{n_1} \cdots L_{n_{M+1}} \rangle_{\beta,R},$$

can be calculated in terms of expectation values with  $M$  and  $M - 1$  operators using cyclicity of the trace and (64) in order to bring  $L_{n_{M+1}}$  cyclically through all other operators. This gives

$$\begin{aligned} \langle L_{n_1} \cdots L_{n_{M+1}} \rangle &= \frac{1}{e^{2\pi\beta n_{M+1}/R} - 1} \sum_{i=1}^M \langle L_{n_1} \cdots [L_{n_{M+1}}, L_{n_i}] \cdots L_{n_M} \rangle \\ &= \frac{1}{e^{2\pi\beta n_{M+1}/R} - 1} \sum_{j=1}^M \left[ (n_{M+1} - n_j) \langle L_{n_1} \cdots L_{n_j+n_{M+1}} \cdots L_{n_M} \rangle (1 - \delta_{n_j+n_{M+1},0}) \right. \\ &\quad \left. + \left( 2n_{M+1} \langle L_{n_1} \cdots L_0 \cdots L_{n_M} \rangle + \frac{c}{12} (n_{M+1}^3 - n_{M+1}) \langle L_{n_1} \cdots \widehat{L}_{n_j} \cdots L_{n_M} \rangle \right) \delta_{n_j+n_{M+1},0} \right], \end{aligned}$$

where in the last line we separated the case where the  $n_i$  and  $n_{M+1}$  add up to zero (and the hat indicates that the factor is omitted). Using (59), this can be re-written as

$$\begin{aligned} \langle a_{p_1}^{(R)} \cdots a_{p_{M+1}}^{(R)} \rangle_{\beta,R} &= \frac{1}{e^{2\pi\beta p_{M+1}} - 1} \sum_{i=1}^M \left[ (p_{M+1} - p_i) \langle a_{p_1}^{(R)} \cdots a_{p_i+p_{M+1}}^{(R)} \cdots a_{p_M}^{(R)} \rangle_{\beta,R} \right. \\ &\quad \left. + 2p_{M+1} \langle a_{p_1}^{(R)} \cdots A^{(R)} \cdots a_{p_M}^{(R)} \rangle_{\beta,R} \right. \\ &\quad \left. + \frac{c}{12} \left( p_{M+1}^3 - \frac{p_{M+1}}{R^2} \right) \langle a_{p_1}^{(R)} \cdots \widehat{a_{p_i}^{(R)}} \cdots a_{p_M}^{(R)} \rangle_{\beta,R} \delta^{(R)}(p_i + p_{M+1}) \right] \quad (69) \end{aligned}$$

and from the induction assumption expressed in (62), we can immediately evaluate the large- $R$  limit:

$$\lim_{R \rightarrow \infty} \langle a_{p_1}^{(R)} \cdots a_{p_{M+1}}^{(R)} \rangle \doteq \frac{1}{e^{2\pi\beta p_{M+1}} - 1} \sum_{i=1}^M \left[ (p_{M+1} - p_i) \langle a_{p_1} \cdots a_{p_i+p_{M+1}} \cdots a_{p_M} \rangle_\beta \right. \\ \left. + \left( 2p_{M+1}k(\beta) + \frac{c}{12}p_{M+1}^3 \right) \langle a_{p_1} \cdots \widehat{a_{p_i}} \cdots a_{p_M} \rangle_\beta \delta(p_i + p_{M+1}) \right]. \quad (70)$$

This is exactly the induction step (39) (along with (34) and (37)) used in order to evaluate averages in the continuous Virasoro algebra. Again this holds for general  $p_i$ s, noting that at  $p_i = 0$  the difference between the left- and right-hand sides are terms that integrate to zero. This shows (62a) for  $M \mapsto M + 1$ .

In order to show (62b) (and similar equations with the operators  $A^{(R)}$  at different positions), one may use again a derivative argument based on (67), and the vanishing, in the large- $R$  limit, of the commutator (68). The fact that the large- $R$  limit commutes with the derivative operator  $\partial/\partial\beta$  can be seen recursively from (69), using the observation that this fact was true in the case  $M = 2$  and using (67) (and again, at every step it is necessary to use this nontrivial fact on the expectation value  $\langle A^{(R)} \rangle_{\beta,R}$ ).

### 5.3 Large $t$ limit

We can now use the results (60) in order to calculate the expectations that appear in the expansion (58). Writing  $S_\tau$  and  $\tilde{S}$  in terms of  $A^{(R)}$  and  $a_p^{(R)}$  following (59), where  $p = n/R$  takes discrete values, we find

$$\tilde{S} = \frac{2\pi t}{R^2} L_0 = 2\pi t A^{(R)} \quad (71a)$$

$$S_\tau = \frac{2}{R} \sum_{n \neq 0} L_n e^{-i\pi n(t+2\tau)/R} \frac{\sin\left(\frac{\pi n t}{R}\right)}{n} = \frac{2}{R} \sum_p a_p^{(R)} e^{-i\pi p(t+2\tau)} \frac{\sin(\pi p t)}{p}. \quad (71b)$$

Equation (60a) then implies that we can express the large  $R$  limit of expectation values of products of  $S_\tau$  in terms of the continuous algebra,

$$\lim_{R \rightarrow \infty} \langle S_{\tau_1} \cdots S_{\tau_M} \rangle_{\beta,R} = 2^M \int d^M p \langle a_{p_1} \cdots a_{p_M} \rangle_\beta \prod_{i=1}^M e^{-i\pi p_i(t+2\tau_i)} \frac{\sin(\pi p_i t)}{p_i}. \quad (72)$$

Further, Equation (60b) and its relatives, i.e. the statement that in the large- $R$  limit,  $A^{(R)}$  becomes central and assumes the fixed value  $k(\beta)$ , implies that in the large- $R$  limit,  $\tilde{S}$  factorizes and can be treated as the number  $2\pi t k(\beta)$ . Therefore, the large- $R$  limit of the expectation value in (57) can be written as

$$\lim_{R \rightarrow \infty} \langle \mathcal{P} \exp \left( \frac{i\Delta\alpha}{\alpha} \int_0^{\lambda\alpha} d\tau (\tilde{S} + S_\tau) \right) \rangle_{\beta,R} \\ = e^{2\pi i t k(\beta) \Delta\alpha \lambda} \sum_{M=0}^{\infty} \left( \frac{2i\Delta\alpha}{\alpha} \right)^M \int d^M p \langle a_{p_1} \cdots a_{p_M} \rangle_\beta \prod_{i=1}^M \int_0^{\tau_i-1} d\tau_j e^{-i\pi p_i(t+2\tau_i)} \frac{\sin(\pi p_i t)}{p_i}, \quad (73)$$

with  $\tau_0 := \lambda\alpha$ .

In order to calculate the large-time cumulant generating function (57), we take the logarithm of the above expression. Recall the combinatoric formula (44): an expectation  $\langle a_{p_1} \cdots a_{p_M} \rangle_\beta$  is a sum over partitions  $S$  of the list of momenta  $(p_1, \dots, p_M)$ , of products over the partition's parts  $s \in S$ ,  $s \subset (p_1, \dots, p_M)$ , of sums  $C(s)$  of connected diagrams linking the momenta in  $s$ . Then by standard combinatoric arguments, the logarithm of (73) is a series formed by the connected averages

$\langle a_{p_1} \cdots a_{p_M} \rangle_\beta^{\text{conn}} := C(p_1, \dots, p_M)$  evaluated by summing over the connected diagrams. From (57) and (73), we have

$$f(\alpha, \Delta\alpha, \beta, \lambda) = 2\pi i k(\beta) \Delta\alpha \lambda + \lim_{t \rightarrow \infty} \frac{1}{t} \sum_{M=2}^{\infty} \left( \frac{2i\Delta\alpha}{\alpha} \right)^M \int d^M p \langle a_{p_1} \cdots a_{p_M} \rangle_\beta^{\text{conn}} \prod_{i=1}^M \int_0^{\tau_i-1} d\tau_i e^{-i\pi p_i(t+2\tau_i)} \frac{\sin(\pi p_i t)}{p_i}. \quad (74)$$

Every connected diagram  $\gamma$  with  $M$  momenta contains exactly one overall delta function  $\delta(p_1 + \cdots + p_M)$ , and can be written in the form

$$G_M^\gamma(\mathbf{p}) \delta(p_1 + \cdots + p_M), \quad (75)$$

where  $G_M^\gamma$ , defined on the hyperplane  $p_1 + \cdots + p_M = 0$ , is an entire function of the momenta except for simple poles when seen as a function of the sum of any subset of the momenta (as is clear from the diagram rules (40a) and (40b)). Hence also connected averages have this form,

$$\langle a_{p_1} \cdots a_{p_M} \rangle_\beta^{\text{conn}} = \left( \sum_{\gamma} G_M^\gamma(\mathbf{p}) \right) \delta(p_1 + \cdots + p_M) =: G_M(\mathbf{p}) \delta(p_1 + \cdots + p_M) \quad (M \geq 2). \quad (76)$$

Taking into account this form, we may evaluate the large-time limit on the right-hand side of (74) using the formula (see e.g. [33])

$$\lim_{t \rightarrow \infty} \frac{1}{t} \int d^M p g(\mathbf{p}) \left( \prod_{i=1}^M \frac{\sin(\pi p_i t)}{\pi p_i} \right) \delta(p_1 + \cdots + p_M) = g(0, \dots, 0), \quad (77)$$

which gives rise to

$$\begin{aligned} f(\alpha, \Delta\alpha, \beta, \lambda) &= 2\pi i k(\beta) \Delta\alpha \lambda + \sum_{M=2}^{\infty} \left( \frac{2\pi i \Delta\alpha}{\alpha} \right)^M G_M(0, \dots, 0) \prod_{i=1}^M \int_0^{\tau_i-1} d\tau_i \\ &= 2\pi i k(\beta) \Delta\alpha \lambda + \sum_{M=2}^{\infty} \frac{(2\pi i \Delta\alpha \lambda)^M}{M!} G_M(0, \dots, 0). \end{aligned} \quad (78)$$

Hence, we need to evaluate  $G_M(0, \dots, 0)$ . Although each  $G_M^\gamma(\mathbf{p})$  has poles which make its value at  $p_1 = \dots = p_M = 0$  ill-defined (the limit of  $G_M^\gamma(\mathbf{p})$  when  $\mathbf{p} \rightarrow (0, \dots, 0)$  does not exist), the sum of all connected diagrams is well defined at zero momenta. The value of  $G_M(0, \dots, 0)$  can be calculated as follows. Consider the operators  $\tilde{a}_p := a_p + k(\beta)\delta(p)$ . These satisfy commutation relations with a central term that does not contain the term linear in  $p$ , that is  $[a_p, a_q] = (p-q) + \frac{c}{12}p^3\delta(p+q)$ . Hence these operators are explicitly independent of  $\beta$ , and they have a nonzero one-point average given by  $\langle \tilde{a}_p \rangle_\beta = k(\beta)\delta(p)$ . Consider the connected averages  $\langle \tilde{a}_{p_1} \cdots \tilde{a}_{p_M} \rangle_\beta^{\text{conn}}$ , defined combinatorically as usual. The insertion of an operator  $\tilde{a}_0$  can be obtained simply by differentiating with respect to  $\beta$ :

$$\langle \tilde{a}_{p_1} \cdots \tilde{a}_{p_M} \tilde{a}_0 \rangle_\beta^{\text{conn}} = -\frac{1}{2\pi} \frac{\partial}{\partial \beta} \langle \tilde{a}_{p_1} \cdots \tilde{a}_{p_M} \rangle_\beta^{\text{conn}}$$

for any  $M \geq 1$ . Since we take connected averages, the shift of the expectation value is irrelevant whenever the number of operator is greater or equal to two:  $\langle \tilde{a}_{p_1} \cdots \tilde{a}_{p_M} \rangle_\beta^{\text{conn}} = \langle a_{p_1} \cdots a_{p_M} \rangle_\beta^{\text{conn}}$  for all  $M \geq 2$ . Hence, we find the recursion relation

$$G_M(0, \dots, 0) = -\frac{1}{2\pi} \frac{\partial}{\partial \beta} G_{M-1}(0, \dots, 0)$$

which holds for all  $M \geq 2$  if we define  $G_1(0) := k(\beta)$ . Using (37), this gives

$$G_M(0, \dots, 0) = \frac{M! k(\beta)}{(2\pi\beta)^{M-1}}.$$

Hence, putting this in (78), we find

$$f(\alpha, \Delta\alpha, \beta, \lambda) = 2\pi\beta k(\beta) \sum_{M=1}^{\infty} \left( \frac{i\Delta\alpha\lambda}{\beta} \right)^M = \frac{2\pi i\beta k(\beta)\Delta\alpha\lambda}{\beta - i\Delta\alpha\lambda}.$$

With (56) and (37), this indeed reproduces (24).

Finally, we observe that the function  $f(\alpha, \Delta\alpha, \beta, \lambda)$  is in fact independent of  $\alpha$ . Hence, seeing our initial expression (46) as a function of  $\alpha_j$  and  $\Delta\alpha_j$  in the form

$$\mathcal{P} \exp \left( i \int_0^\lambda d\lambda' e^{i\lambda'Q(\{\alpha\})} (\Delta_t Q)(\{\Delta\alpha\}) e^{-i\lambda'Q(\{\alpha\})} \right),$$

we conclude that the same result for the full counting statistics is obtained by setting  $\alpha_j = 0$  in this expression. But setting  $\alpha_j = 0$  means setting  $Q = 0$ , and the exponential becomes simply  $e^{i\lambda\Delta_t Q}$ , so that we have shown that the expression (21) indeed gives the same result.

## 5.4 UV regularization

In the above derivation, we omitted the explicit momentum cutoff  $\Lambda$  in our integrals. These cutoffs are necessary because the expression (72), for the large- $R$  limit of expectation values at finite time  $t$ , is a multiple momentum integral that is divergent at large momenta. In fact, as we mentioned, even before taking the large- $R$  limit, at each order in  $\lambda$ , the average of  $e^{i\lambda Q(t)} e^{-i\lambda Q}$ , written in terms of sums over Virasoro indices  $n_i$  of averages of Virasoro generators through (55), (53) and (54), is divergent at large values of  $n_i$ . These divergencies are expected, as we are effectively evaluating exponentials of local fields (integrated over finite regions) in a quantum field theory. Hence, in order to make our calculations finite, we need a UV regularization. A natural way of regularizing is to modify the expression of the local fields needed,  $h^{(j,j+1)}(x)$ : as was done above, one may simply sum over indices  $n \in \mathbb{Z} \cap [-\mathcal{N}, \mathcal{N}]$  in (50), with  $\mathcal{N} > 0$  finite. Then the finite- $R$  average of  $e^{i\lambda Q(t)} e^{-i\lambda Q}$ , which is the average of path-ordered exponential (55), is finite order by order in  $\lambda$ . At large  $R$ , however, we need to make sure that the UV regularization, which should be an energy, behaves correctly: what needs to be fixed is not the range of the dimensionless indices  $n$ , but rather the range of the momenta  $p$ . That is, we take  $\mathcal{N} = \Lambda R$  with  $\Lambda$  a fixed quantity with dimension of energy. Then, the regularization translates into limiting the multiple momentum integral to the range  $p_i \in [-\Lambda, \Lambda]$  in (72), which is indeed finite. The large- $t$  limit can then be taken, which kills the integral and constrains the values of the momenta to 0. Hence after the large- $t$  limit is taken, the result is explicitly independent of  $\Lambda$ : the UV regularization can be taken to infinity.

These considerations, and our proof above, gives further confirmation of the claim made in [8, 9] that the result for the full counting statistics of the energy flow in CFT is universal (although it is not a proof and doesn't fully address the problem of irrelevant operators). Indeed, we have here a very different regularization scheme (perhaps more standard) than that used in [9], yet we find the same result.

The present considerations can also be translated into an intuition as to how the special steady-state limit,  $R \rightarrow \infty$  followed by  $t \rightarrow \infty$ , behaves in terms of the Virasoro modes in CFT. Indeed, as we mentioned, the present formulation is equivalent to a two-time measurement where the first measurement is at the connection time. Hence, although the parameter  $R$  we used was an ‘‘artefact’’ in order to construct the steady-state density matrix, it can be interpreted as the length of the physical system; and the time  $t$  between the two measurements can be interpreted as the time the system has evolved towards the steady state. Then, the way we took the  $R \rightarrow \infty$  limit indicates that the large-volume physics occurs at very large modes,  $n \sim pR$  with fixed momenta  $p$ , and the result of the  $t \rightarrow \infty$  limit indicates that the large-time limit is dominated by very small values of momenta  $p$ .

## 6 Conclusion

We have evaluated the scaled cumulant generating function for the energy transfer in NECFT on a star graph with temperature imbalances amongst the legs of the graph, and a simple connection condition at the vertex. We introduced new techniques in order to perform the calculation, in particular studying a continuous version of the Virasoro algebra and the associated diagrams. This generalizes the NECFT results of [8, 9] to the star-graph configuration, and agrees, in the particular case of unit central charge, with previously obtained results concerning free bosons (Luttinger liquids) [29] and free Dirac fermions [27] on star graphs. Our results further confirm the universality of the NECFT full counting statistics, as well as the Poisson-process picture underlying long-time energy transfer in NECFT.

There are interesting open problems that the techniques of the present paper may help address. An immediate question concerns the energy or charge transfer in the cases of a nontrivial but conformal impurity at the vertex of the graph. Since impurities are usually described algebraically in CFT, it is possible that the present Virasoro-algebraic methods may be of use in order to make progress. Another set of non-equilibrium problems that are of current interest are those where parameters of a system are suddenly changed and the system then let to evolve. It is expected that the result at large time is a so-called “generalized Gibbs ensemble”, described by a nontrivial density matrix. The techniques developed here may help in evaluating averages in such density matrices. Finally, it would also be interesting to generalize the present ideas to non-conformal (say integrable) situations, for instance with conformal baths and a non-conformal integrable impurity (like the multi-channel Kondo model).

## A Comparison with other results

We compare our results for the energy current with the results obtained in [27], where the steady charge and energy current were obtained for a quantum wire junction (both relativistic and nonrelativistic). The quantum junction is modeled by a star graph where fields living on one of the legs that are incoming to the vertex have an associated temperature and chemical potential determined by the leg. The charge and energy exchange are modeled by pointlike interactions in the vertex, and for comparison with our results, we take these to be scale-invariant. In the notation of [27] this means the scattering matrix takes the form

$$\mathbb{S}_{\text{inv}} = \theta(k)\mathbb{U} + \theta(-k)\mathbb{U}^{-1}, \quad (79)$$

where in [27] the matrix  $\mathbb{U}$  is an arbitrary unitary  $N \times N$  matrix, representing the vertex conditions for positive or negative values of the parameter  $k$  (which plays the role of a momentum). We note that the diagonal elements are reflection at the vertex, and off-diagonal element  $\mathbb{S}_{ij}$  is the transmission amplitude from the  $i$ -th leg to the  $j$ -th leg. This means that the vertex conditions of the present work correspond to the following choice for  $\mathbb{U}$ ,

$$\mathbb{U}_{ij} = \alpha_{i-1} \delta_{j,i-1}, \quad \mathbb{U}_{ij}^{-1} = \alpha_i^{-1} \delta_{j,i+1}, \quad (80)$$

with the requirement

$$\alpha_j^{-1} = \alpha_j^*. \quad (81)$$

The energy flow from the  $i$ -th leg into the vertex at criticality is given by

$$\mathcal{T}_i(\beta, \mu, \tilde{\mu}) = \frac{1}{2\pi} \sum_{j=1}^N (|\mathbb{U}_{ij}|^2 - \delta_{ij}) \frac{1}{\beta_j^2} [\text{Li}_2(-e^{-\beta_j \mu_j}) + \text{Li}_2(-e^{-\beta_j \tilde{\mu}_j})] \quad (82)$$

With  $\text{Li}_2(x)$  known as the dilogarithm (or Spence function  $\text{Sp}(x)$ ). Since we assume that the chemical potentials for the (anti)particles are all equal, we may take them to zero, and the terms between

square brackets become:

$$\text{Li}_2(-e^{-\beta_j \mu_j}) + \text{Li}_2(-e^{-\beta_j \tilde{\mu}_j}) \Big|_{\mu, \tilde{\mu}=0} = 2\text{Li}_2(-1) = -\frac{2\pi^2}{12}. \quad (83)$$

The heat flow for zero chemical potential is given by,

$$\mathcal{T}_i(\beta) = \frac{\pi}{12} \sum_{j=1}^N (\delta_{ij} - |\mathbb{U}_{ij}|^2) \frac{1}{\beta_j^2}. \quad (84)$$

For our example of sequentially connected CFTs, we have

$$|\mathbb{U}_{ij}|^2 = \mathbb{U}_{ij}^* \mathbb{U}_{ij} = \alpha_{i-1}^* \alpha_{i-1} \delta_{j,i-1} = \alpha_{i-1}^{-1} \alpha_{i-1} \delta_{j,i-1} = \delta_{j,i-1}, \quad (85)$$

so the heat flow at criticality from the  $i$ -th leg into the  $i+1$ -th leg is given by

$$\mathcal{T}_i(\beta) = \frac{\pi}{12} \left( \frac{1}{\beta_i^2} - \frac{1}{\beta_{i-1}^2} \right). \quad (86)$$

Summing over all legs, and giving each contribution a weight  $\Delta\alpha_i$ , it is easy to see that this agrees with our result (19), with a choice of the central charge  $c = 1$ .

## B An operator interpretation of the change of connection at the vertex of the graph

At the time  $-t_0$  when the  $N$  separate systems are connected as represented in Figure 2, there is a drastic change in the dynamics. Such changes of boundary or ‘‘impurity’’ conditions are often represented in CFT as insertions of particular local fields at the position of the impurity. Although this picture is a Euclidean one, and doesn’t seem to be directly applicable to the calculation of quantities in the non-equilibrium steady state, it may be of use in evaluating overlaps between Hamiltonian eigenstates before and after the connection.

In the present context, there is a very natural interpretation of the impurity changing operator. Indeed, before the connection we have  $N$  independent chiral copies of a CFT model, while at the moment of the connection, these copies are connected to each other in a sequential way. Geometrically, this means that at the time of the connection there is a branch point. Hence, the impurity condition changing operator should be the branch-point twist field, a twist field associated to the  $\mathbb{Z}_N$  symmetry of any model composed of  $N$  independent copies. An elegant derivation of its scaling dimension was found in [35] in the context of evaluating the entanglement entropy in CFT.

This can be confirmed by analyzing the shift of  $L_0$ -eigenvalues produced by the connection, which should be related to the dimension of the branch-point twist field. This shift is easily calculated as follows. Consider the total energy before and after the connection. Before the connection, there are  $N$  independent Virasoro algebras,  $L_n^{(j)}$ ,  $n \in \mathbb{Z}$ , representing the single chiral fields running around each leg of the graph. In each leg  $j$ , a single chiral field is used, as is standard in boundary CFT, to represent both  $h_j^{\text{in}}(x)$  and  $h_j^{\text{out}}(x)$  and the reflecting boundary conditions at  $x = 0$  and  $x = R$ . After the connection, there is a single Virasoro algebra  $L_n$ ,  $n \in \mathbb{Z}$ , representing the single chiral field running around the whole graph, see the left part of Figure 2. This single chiral field now represents all of the fields  $h_j^{\text{in}}(x)$  and  $h_j^{\text{out}}(x)$ , for  $j = 1, \dots, N$ , as well as the special connection at the vertex of the graph. Denoting  $\tilde{L}_n = L_n - \frac{c}{24}\delta_{n,0}$  and  $\tilde{L}_n^{(j)} = L_n^{(j)} - \frac{c}{24}\delta_{n,0}$ , the energy before the connection is the sum of those of the  $N$  separate systems, each of length  $R$ :

$$\frac{2\pi}{R} \sum_{j=1}^N \tilde{L}_0^{(j)}.$$

After the connection, the energy is that of a single system, but of length  $NR$ ,

$$\frac{2\pi}{NR} \tilde{L}_0.$$

Since the connection only changes the energy by an infinitesimal amount, these should be equal,

$$\frac{1}{N}L_0 + \frac{c}{24} \left( N - \frac{1}{N} \right) = \sum_{j=1}^N L_0^{(j)}. \quad (87)$$

Hence, the eigenvalues of  $\sum_{j=1}^N L_0^{(j)}$ , in the initial system, are shifted by  $d := \frac{c}{24} \left( N - \frac{1}{N} \right)$  as compared to the eigenvalues of  $\frac{1}{N}L_0$  (the  $1/N$  scaling simply represents the change of length). The number  $d$  is indeed the holomorphic dimension of the branch-point twist field [35].

Relation (87) is one of an infinity of relations amongst the Virasoro generators before and after the connection. These relations can be obtained as follows. Consider a local right-moving energy density  $h_+(z)$ , for  $z \in [0, NR]$  running over the chiral paths of all legs of the graph. Before the connection,  $h_+(z)$  is interpreted as representing the chiral fields in all separate legs, with each leg corresponding to an interval  $z \in [jR, (j+1)R]$  of length  $R$ , and with periodicity given by identifying the points  $z = j$  and  $z = j+R$ , for  $j = 0, \dots, N-1$ . After the connection, the same field  $h_+(z)$  is now interpreted as representing a single chiral field on the interval of length  $NR$ , with periodicity where the point 0 is identified with the point  $NR$ . The field  $h_+(x)$  can then be written in two different ways:

$$\begin{aligned} h_+(z) &= \frac{2\pi}{R^2} \left( -\frac{c}{24} + \sum_{n \in \mathbb{Z}} L_n^{(j)} e^{2\pi i n z / R} \right) \Theta(jR \leq z < (j+1)R) \\ &= \frac{2\pi}{R^2} \left( -\frac{c}{24} + \sum_{n \in \mathbb{Z}} L_n e^{2\pi i n z / (NR)} \right) \end{aligned}$$

where  $\Theta(\dots)$  is one if the condition  $\dots$  is satisfied, and zero otherwise. The equality between these two expressions gives rise to an infinity of relations between  $L_n$  and  $L_n^{(j)}$ . In particular, one family of such relations is

$$\frac{1}{N}L_{Nk} + \frac{c}{24} \left( N - \frac{1}{N} \right) \delta_{k,0} = \sum_{j=1}^N L_k^{(j)}, \quad k \in \mathbb{Z}$$

which generalizes (87). It is indeed a simple matter to check that both sides are generators that satisfy the Virasoro algebra commutation relations with central charge  $Nc$ .

## References

- [1] R. Zwanzig. *Nonequilibrium statistical mechanics*. Oxford University Press, USA, 2001.
- [2] Y. Utsumi, D. Golubev, M. Marthaler, K. Saito, T. Fujisawa, and G. Schön. Bidirectional single-electron counting and the fluctuation theorem. *Phys. Rev. B*, 81(12):125331, 2010.
- [3] S. Nakamura, Y. Yamauchi, M. Hashisaka, K. Chida, K. Kobayashi, T. Ono, R. Leturcq, K. Ensslin, K. Saito, Y. Utsumi, et al. Nonequilibrium fluctuation relations in a quantum coherent conductor. *Phys. Rev. Lett.*, 104(8):080602, 2010.
- [4] S. Nakamura, Y. Yamauchi, M. Hashisaka, K. Chida, K. Kobayashi, T. Ono, R. Leturcq, K. Ensslin, K. Saito, Y. Utsumi, et al. Fluctuation theorem and microreversibility in a quantum coherent conductor. *Phys. Rev. B*, 83(15):155431, 2011.
- [5] R. Sánchez and M. Büttiker. Detection of single-electron heat transfer statistics. *Europhys. Lett.*, 100(4):47008, 2012.



- [6] O.-P. Saira, Y. Yoon, T. Tantt, M. Möttönen, D. Averin, and J. Pekola. Test of the Jarzynski and Crooks fluctuation relations in an electronic system. *Phys. Rev. Lett.*, 109(18):180601, 2012.
- [7] M. Esposito, U. Harbola, and S. Mukamel. Nonequilibrium fluctuations, fluctuation theorems, and counting statistics in quantum systems. *Rev. Mod. Phys.*, 81(4):1665, 2009.
- [8] D. Bernard and B. Doyon. Energy flow in non-equilibrium conformal field theory. *J. Phys. A*, 45(36):362001, 2012.
- [9] D. Bernard and B. Doyon. Non-equilibrium steady-states in conformal field theory. arXiv:1302.3125.
- [10] C. Karrasch, R. Ilan and J. E. Moore. Nonequilibrium thermal transport and its relation to linear response. arXiv:1211.2236
- [11] P. Kuchment. Quantum graphs: an introduction and brief survey. In: *Analysis on Graphs and Its Applications*, Exner, P. et al. (eds), Proc. Symp. Pure Math. vol 77, p. 291, 2008.
- [12] C. Nayak, M. Fisher, A. Ludwig, and H.-H. Lin. Resonant multi-lead point-contact tunneling. *Phys. Rev. B*, 59:15694, 1999.
- [13] M. Oshikawa, C. Chamon, and I. Affleck. Junctions of three quantum wires. *J. Stat. Mech.*, 0602:P02008, 2006.
- [14] C.-Y. Hou, E.-A. Kim, and C. Chamon. Corner junction as a probe of helical edge states. *Phys. Rev. Lett.*, 102:076602, 2009.
- [15] A. Agarwal, S. Das, S. Rao, and D. Sen. Enhancement of tunneling density of states at a junction of three Luttinger liquid wires. *Phys. Rev. Lett.*, 103:026401, 2009.
- [16] I. Safi, P. Devillard, and T. Martin. Partition noise and statistics in the fractional quantum Hall effect. *Phys. Rev. Lett.*, 86(20):4628, 2001.
- [17] B. Béri, and N.R. Cooper. Topological Kondo effect with Majorana fermions. *Phys. Rev. Lett.*, 109:156803, 2012.
- [18] A.M. Tsvelik. Majorana fermion realization of 2-channel Kondo effect in a junction of three quantum Ising chains. arXiv:1211.3481
- [19] N. Crampé, and A. Trombettoni. Quantum spins on star graphs and the Kondo model. *Nucl. Phys. B*, 871 [FS]: 526, 2013
- [20] D. Friedan. Entropy flow in near-critical quantum circuits. arXiv:cond-mat/0505084. Entropy flow through near-critical quantum junctions. arXiv:cond-mat/0505085.
- [21] S. Das, S. Rao and D. Sen. Interedge interactions and fixed points at a junction of quantum Hall line junctions. *Phys. Rev. B*, 74:045322, 2006.
- [22] B. Bellazzini and M. Mintchev. Quantum fields on star graphs. *J. Phys. A*, 39:11101, 2006.
- [23] B. Bellazzini, M. Mintchev, and P. Sorba. Bosonization and scale invariance on quantum wires. *J. Phys. A*, 40:2485, 2007.
- [24] B. Bellazzini, M. Burrello, M. Mintchev, and P. Sorba. Quantum field theory on star graphs. In: *Analysis on Graphs and Its Applications*, Exner, P. et al. (eds), Proc. Symp. Pure Math. vol 77, p. 639, 2008.
- [25] E. Ragoucy. Quantum field theory on quantum graphs and application to their conductance. *J. Phys. A*, 42:295205, 2009.

- [26] A. Rahmani, C.-Y. Hou, A. Feiguin, M. Oshikawa, C. Chamon, and I. Affleck. General method for calculating the universal conductance of strongly correlated junctions of multiple quantum wires. *Phys. Rev. B*, 85:045120, 2012.
- [27] M. Mintchev. Non-equilibrium steady states of quantum systems on star graphs. *J. Phys. A*, 44(41):415201, 2011.
- [28] V. Caudrelier, M. Mintchev, and E. Ragoucy. Quantum wire network with magnetic flux. *Phys. Lett. A*, 377:1788, 2013.
- [29] M. Mintchev and P. Sorba. Luttinger liquid in non-equilibrium steady state. *J. Phys. A*, 46:095006, 2013.
- [30] V. Caudrelier and E. Ragoucy. Direct computation of scattering matrices for general quantum graphs. *Nucl. Phys. N*, 828:515, 2009.
- [31] J. Cardy. Conformal Invariance and Surface Critical Behavior. *Nucl. Phys. B*, 240 [FS12]: 514, 1984.
- [32] L.S. Levitov and G.B. Lesovik. Charge distribution in quantum shot noise. *JETP Lett.* 58:230, 1993.
- [33] D. Bernard and B. Doyon. Full counting statistics in the resonant-level model. *J. Math. Phys.*, 53(12):2302, 2012.
- [34] P. Di Francesco, P. Mathieu, and S. Senechal. *Conformal Field Theory*, Springer:Berlin, 1997.
- [35] P. Calabrese and J. L. Cardy, Entanglement entropy and quantum field theory, *J. Stat. Mech.* P06002, 2004.